# RAPID ESTIMATION OF LYCOPENE CONCENTRATION IN WATERMELON AND TOMATO SAMPLES BY FIBER OPTIC VISIBLE SPECTROSCOPY

By

RUPLAL CHOUDHARY

Bachelor of Technology
Jawaharlal Nehru Agricultural University,
Jabalpur, India
1991

Master of Technology
Indian Institute of Technology,
Kharagpur, India
1994

Submitted to the faculty of the
Graduate college of the
Oklahoma State University
In partial fulfillment of
The requirement for
The Degree of
DOCTOR OF PHILOSOPHY
December, 2004

RAPID ESTIMATION OF LYCOPENE

CONCENTRATION

IN WATERMELON AND TOMATO SAMPLES

BY FIBER OPTIC VISIBLE SPECTROSCOPY

Thesis Approved:

Thesis Advisor: Dr. Timothy J. Bowser

Chairman: Dr. Marvin L. Stone

Member: Dr. Paul R. Weckler

Member: Dr. Niels O. Maness

Member: Dr. William G. McGlynn

Dean of the Graduate College: Dr. Al Carlozzi

**Acknowledgement**

It was my great pleasure and honor to be a graduate student of my advisor and mentor Dr. Timothy J. Bowser. He always kept me focused in my research while allowing me to develop myself as an independent researcher. His encouragement for collaborative research helped me to interact with experts not only on campus but around the globe. I sincerely thank him for his financial, moral and intellectual support during my doctoral study.

I am highly thankful to Dr. Paul Weckler, who has not only provided me intellectual guidance but also funded my research project. His enthusiasm for achieving excellence in agricultural sensing encouraged me to select my research project in lycopene sensing. It is because of his support and encouragement that I could pursue cutting edge research in Biosystems Engineering. It was my great pleasure to interact with Dr. Niels O. Maness from the department of Horticulture and Landscape Architecture. He was not only my committee member but also an active research collaborator. His level of curiosity and enthusiasm helped me shape my research objectives. I am thankful to him for providing me unlimited access to his lab for chemical analysis. I am highly thankful to Dr. Marvin Stone for chairing my advisory committee and providing fiber optic sensing facility. His critical reviews and constructive suggestions were very helpful in perfecting this dissertation. I want to convey my sincere

thanks to Dr. William McGlynn for being friendly and supportive of my research approach.

I am thankful to Dr. Ronald Elliot, Head, Biosystems and Agricultural Engineering (BAE) and Dr. Gerald Brusewitz, professor emeritus, whose constant encouragement and support helped me continue my studies in the department against all odds. Thanks to the BAE staff members for making my stay in the department smooth and pleasant. Sincere thanks to Mr. Wayne Kiner and staff members of BAE Workshop for timely fabrication of research equipment. Thanks to Mr. David Moe, Pilot Plant Manager, Food and Agricultural Products Research and Technology Center for help in watermelon slicing. Special thanks to Dr. Carla Goad for help in statistical analysis using SAS software.

It was my great luck to get in touch with Dr. Glenn Kranzler and obtain his help in improving my writing skills. His sincere concerns for my professional and personal growth have deeply touched me and made me more confident in my professional career.

I am thankful to fellow graduate students, Dr. Nachiket Kotwaliwale, Dr. Jeyam Subbiah, Mr. Rajesh Soni, Mr. Aswin Ramachandran, Mr. Tesfaye Demissie, and many other friends who were helpful during my research and dissertation writing.

I am highly indebted to my wife Deepika, and daughters Riddhi and Roshni, for their sacrifice, love and patience during my stay in U.S.A. for pursuing my Ph.D. I am thankful to my beloved parents who encouraged me to be focused in my studies and accomplish my goal.

Last but not least, I am thankful to the Stillwater community for providing me a pleasant and conducive atmosphere for research and study.

## Table of Contents

Chapter Page

Chapter Page

Chapter Page

## List of Tables

Table Page

## List of Figures

Figure Page

## Nomenclature

A - Absorbance

$A_\lambda$ - Absorbance at wavelength $\lambda$

$A_R$ - Apparent absorbance (in reflectance mode)

AI - Absorbance Index

dist - Center to center distance between source and detector optical fibers

lyco - Lycopene concentration, μg/g

LS - Least Squares

NA - Normalized Absorbance

*na* - Numerical aperture

NAI - Normalized Absorbance Index

nm - Nanometer

PLS - Partial Least Squares

R - Measured reflectance

$R_a$ - Actual reflectance

$R_\infty$ - Reflectance from an infinitely thick sample (a thickness of material which does not transmit light through it)

$R^2$ - Coefficient of Determination

SEC - Standard Error of Calibration

SEV - Standard Error of Validation

μg/g - Micrograms per gram

# 1 INTRODUCTION

Lycopene is the red pigmenting compound of watermelon and tomato. It received significant attention after a clinical study on human subjects found strong negative correlation between lycopene in blood serum and the occurrence of prostate cancer (Giovannucci et al., 1995). Since then, several additional studies on the health benefits of lycopene have found that the regular consumption of a lycopene rich diet can prevent some cancers and cardiovascular diseases (Agarwal and Rao, 2000; Astorg, 1997; Clinton, 1998; Gerster, 1997; Masaev, et al., 1997; Weisburger, 1998). Lycopene is the most prevalent carotenoid of the human blood stream and is found in numerous organs such as the prostate, testicles, adrenal gland, pancreas, liver, breast, and skin (Rao and Agarwal, 1999).

Lycopene is a highly unsaturated hydrocarbon, $C_{40}H_{56}$, of the carotenoid family. Due to its molecular structure, lycopene and other carotenoids react rapidly with oxidizing agents and free radicals. As a result, carotenoids act as natural antioxidants. Lycopene is the most potent antioxidant among carotenoids as it has the highest singlet oxygen quenching rate of all the carotenoids found in biological systems (Di Mascio et al., 1989; Tinker et al., 1994).

Due to the increasing popularity of lycopene as one of the important nutraceuticals for use in food and nutritional supplements, scientists are interested in developing lycopene rich products and ingredients by extracting and using lycopene from

watermelon and tomato. The process of recovery and use of lycopene requires measurement of lycopene in raw materials, processes and products. Present methods of lycopene assay require extraction of lycopene from samples in hazardous organic solvents, and are time consuming, tedious, hazardous and destructive. Therefore, these lycopene assay methods are not suitable for fast lycopene estimation required in the field and for on-line processes. A rapid method for lycopene quantification in raw materials and products is urgently required, which should be portable and easily usable in the field and in food and nutraceutical processing industries.

Although lycopene may be available in small quantities in apricot, pink fleshed guava, and pink grapefruit (Mangels et al., 1993), its major natural sources are watermelon and tomato (USDA-NCC, 1998; Holden et al., 1999). Lycopene concentration in red-fleshed watermelon of different cultivars can be as low as 12 μg/g in some seeded cultivars to 100 μg/g in some individual seedless watermelons (Tomes et al., 1963; Perkins-Veazie et al., 2001). Lycopene concentration in fresh tomatoes may vary from 5 to 50 μg/g, depending on the cultivar, ripening stage, and temperature during crop growth (Scott et al., 1995; Cadoni et al., 2000; Hadley et al., 2002).

Most of the studies of lycopene asssay methods have been conducted using tomatoes (Beerh and Sidappa, 1959; Adsule and Dan, 1979; Sadler et al., 1990; D'Souza et al., 1992; Arias et al., 2000.). However, recently there have been some studies on lycopene assay in watermelon (Fish et al., 2002; Perkins-Veazie et al., 2001; Davis et al., 2003a and 2003b). The majority of lycopene assay studies focused on methods involving extraction in organic solvents followed by use of either a spectrophotometer or a High Performance Liquid Chromatograph (HPLC).

Some studies have looked at developing non-extraction methods by using chromaticity of tomatoes (D'Souza et al., 1992) and tristimulus color reading of cut watermelons (Perkins-Veazie et al., 2001), but no reliable methods were found to replace chemical extraction methods.

Recently, Davis et al. (2003a, 2003b) developed a color absorbance method for lycopene assay of watermelon and tomato puree. They used a xenon flash colorimeter/spectrophotometer to obtain color absorbance spectra of watermelon and tomato puree. Absorbance at 700 nm was subtracted from absorbance at 560 nm for correlation with lycopene content. A good linear correlation ($R^2 = 0.98$) was found between absorbance difference (560nm - 700nm) and lycopene content. They reported a mean standard error of correlation of 2.85% for watermelon puree and 14.4 % for tomato puree. Though this study was a serious attempt to develop a reagentless lycopene quantification technique, the spectrometer used in this study had an integrating sphere type sensing unit, which is inherently bulky and is best suited for a laboratory setup.

An economical, fast and miniature sensing device is desired to implement a rapid lycopene sensing technique in the field, and in food and nutraceutical processes. Fiber optic probes offer an advantage of small size and may be readily installed in a process line or equipment for continuous monitoring. They also offer the advantage of portability and may easily be deployed for lycopene sensing in the field.

## 1.1 OBJECTIVES

The overall goal of this study was to use fiber optic spectral sensing techniques for measuring lycopene concentration in watermelon and tomato samples. The three specific objectives were as follows:

1. Correlate the optical reflectance and transmittance spectra of watermelon flesh to its lycopene concentration.
2. Correlate the reflectance spectra of pureed samples of watermelon and tomato with their lycopene concentrations.
3. Find the effect of lycopene concentration and the distance of separation between the source and detector fiber optics on Absorbance Index (AI) and Normalized Absorbance Index (NAI).

# 2 REVIEW OF LITERATURE

This chapter presents some theoretical background and review of literature on lycopene quantification methods. A comprehensive review of chemical and physical properties of lycopene, its synthesis in plants cells and stability during processing and storage is presented. Current lycopene assay techniques and their advantages and disadvantages are discussed. Review of visible spectroscopy as a chemical sensing technique is presented. Use of fiber optic sensors in visible spectroscopy is discussed. Techniques of multivariate statistical analysis as a spectral analysis tool are presented in brief.

## 2.1 CHEMICAL STRUCTURE AND PROPERTIES OF LYCOPENE

Lycopene is a highly unsaturated hydrocarbon of the carotenoid family with an empirical formula of $C_{40}H_{56}$ and a molecular weight of 537. The chemical structure of lycopene is as shown in figure 2.1 below.

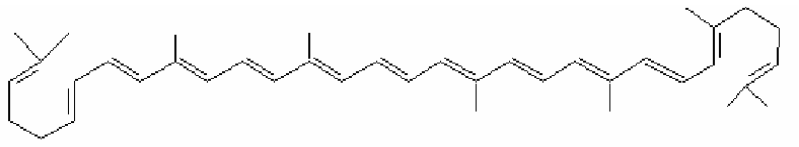

**Figure 2.1: Chemical Structure of Lycopene**

The most characteristic feature of a carotenoid structure is the long polyene chain of alternating double and single bonds that form the central part of the molecule. This feature, called a conjugated structure, gives the carotenoids their distinctive molecular

shape, chemical reactivity, and light absorbing properties (Britton, 1995a; Olson and Krinsky, 1995). Because of isomerism around the C=C double bonds, different configurations of the carotenoid structures are possible. Therefore, lycopene can be found in both *cis* or *trans* forms. In principle, each double bond in the polyene chain of a carotenoid can exist in either of *cis* or *trans* form, making it possible to have a large number of mono*cis* and poly*cis* isomers. However, in reality, only a few of the isomers are encountered in nature since the presence of a *cis* double bond creates greater steric hinderance between nearby hydrogen atoms or methyl groups, so the *cis* isomers are generally less stable than the *trans* forms. Most carotenoids including lycopene, occur in nature predominantly in the all-*trans* form. In fresh watermelon and tomatoes, above 90% of the lycopene is available in *trans* form (Collins, 2003). Though most plant sources have *trans* forms of lycopene, the majority of lycopene in human blood exists as *cis* form. (Boileau et al., 2002). *Cis*-isomers are less likely to crystallize or aggregate and are consequently more readily solubilized, absorbed and transported than their all-*trans* forms (Olson and Krinsky, 1995).

Lycopene molecules are extremely hydrophobic with very low solubility in water. Therefore, they are expected to be restricted to hydrophobic areas in the cells, such as the inner core of membranes, except when association with protein that allows them access to aqueous environments. Lycopene and other carotenoids are natural antioxidants that react rapidly with oxidizing agents and free radicals. Lycopene has the highest singlet oxygen quenching rate of all carotenoids in biological systems (Di Mascio et al., 1989, Tinker et al., 1994).

## 2.2 LYCOPENE CONTENTS OF WATERMELON AND TOMATO

Tomato and watermelon are two major natural sources of lycopene. Though a few red fruits and vegetables such as pink grapefruit and guava contain detectable quantities of lycopene, red fleshed watermelon on average contains higher levels of lycopene per serving than other fresh fruit or vegetable (USDA-NCC 1998). The edible portion of raw red watermelon has an average of 45.32 μg/g lycopene compared to 25.73 μg/g (on average) in the edible portion of tomato (USDA, 2004). Lycopene content in watermelon varies greatly depending on cultivars and growing conditions (Perkins-Veazie et al., 2001). Tomes et al. (1963) found red-fleshed watermelon of different cultivars varied in lycopene concentration from 12.2 to 52.5 μg/g. Lycopene concentration in commercial watermelons has been reported to be 45.1 to 53.2 μg/g (Mangels et al., 1993). Perkins-Veazie et al. (2001), found that the average lycopene content of red-fleshed 'seedless' watermelon cultivars varied from 57.4 - 71.2 μg/g. In the same study, the lycopene values for individual melons ranged between 25 to 100 μg/g.

Tomato and tomato-based products are the major source of lycopene in the American diet (Mangles et al., 1993; Scott et al., 1995). Lycopene concentration in fresh tomatoes can vary from 5 to 50 mg/g, depending on variety, ripening stage, and temperature during growth (Scott et al., 1995; Cadoni et al., 2000; Hadley et al., 2002).

## 2.3 BIOSYNTHESIS OF LYCOPENE IN WATERMELON AND TOMATO

Lycopene biosynthesis is plant cells have been explained by metabolic pathway of carotenoid synthesis in a model plant, *Arabidopsis thaliana* (Goodwin, 1980). A carotenoid pathway is shown in figure 2.2.

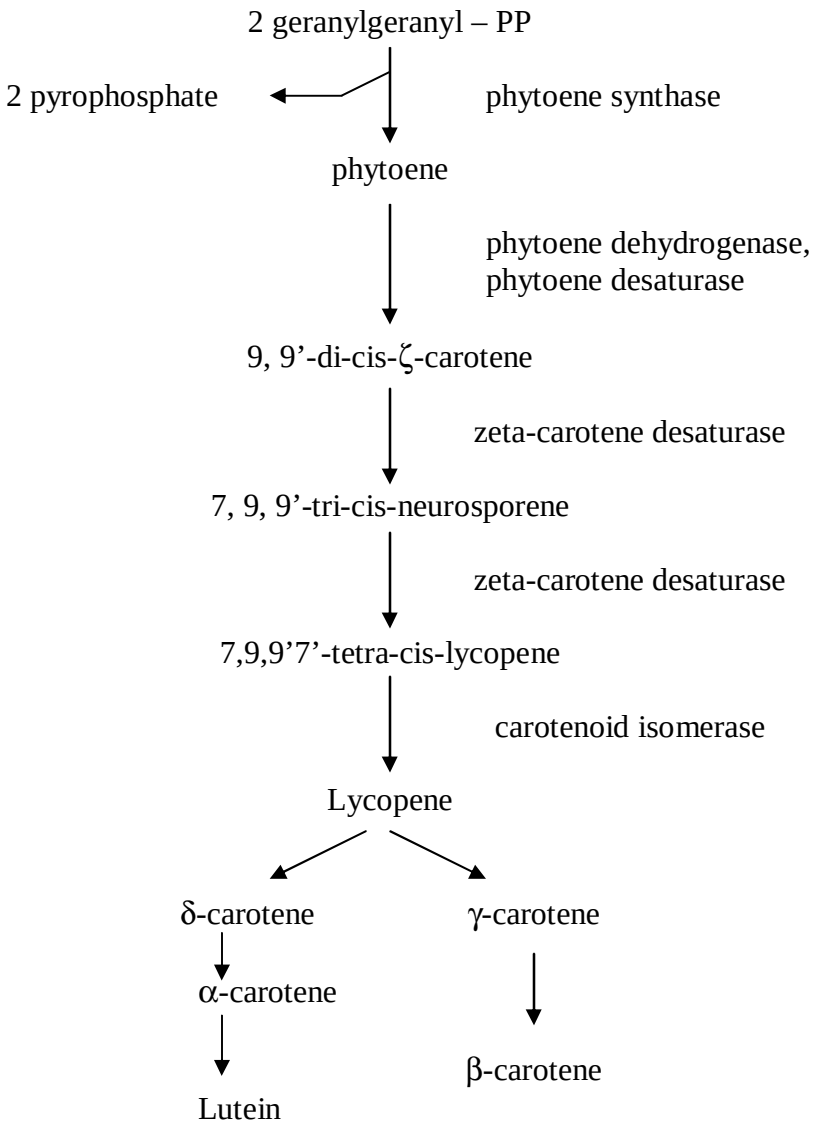


**Figure 2.2: Metabolic pathway for biosynthesis of lycopene and other carotenoids (Goodwin, 1980; MetaCyc Database, 2002)**

The first step specific to the pathway of carotenoid biosynthesis is the production of the symmetrical 40-carbon phytoene from 20-carbon geranylgeranyl pyrophosphate. Phytoene then undergoes a series of four desaturation steps to form first phytofluene and then, in turn, ζ(zeta)-carotene, neurosporene, and lycopene. Cyclization reactions at each

end of the lycopene molecule result in the formation of β-carotene, which may then serve as the substrate for production of the xanthophylls (oxygenated carotenoids). Thus lycopene is a precursor of β-carotene and lutein. Due to the common pathway of synthesis of carotenoids, other carotenoids may also be available in small quantities in watermelon and tomatoes and may interfere in spectral measurement of lycopene in these fruits.

Cross sections of tomato and watermelon are shown in figures 2.3 and 2.4 respectively. Lycopene is synthesized in chromoplasts of fruit cells. Most of the cells in the pericarp near the epidermis synthesize higher lycopene levels than the inner tissue of tomatoes (Sharma and Le Maguer, 1999). In tomatoes, full ripening takes place 40-60 days after planting, during which chloroplasts change to chromoplasts upon synthesis of lycopene. In watermelon, the chromoplasts develop with biosynthesis of lycopene in mesocarp cells.

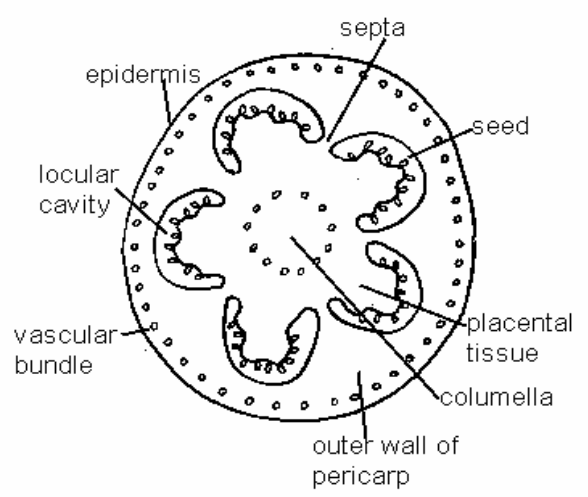


**Figure. 2.3: Cross section of tomato fruit (Rost, 1996)**

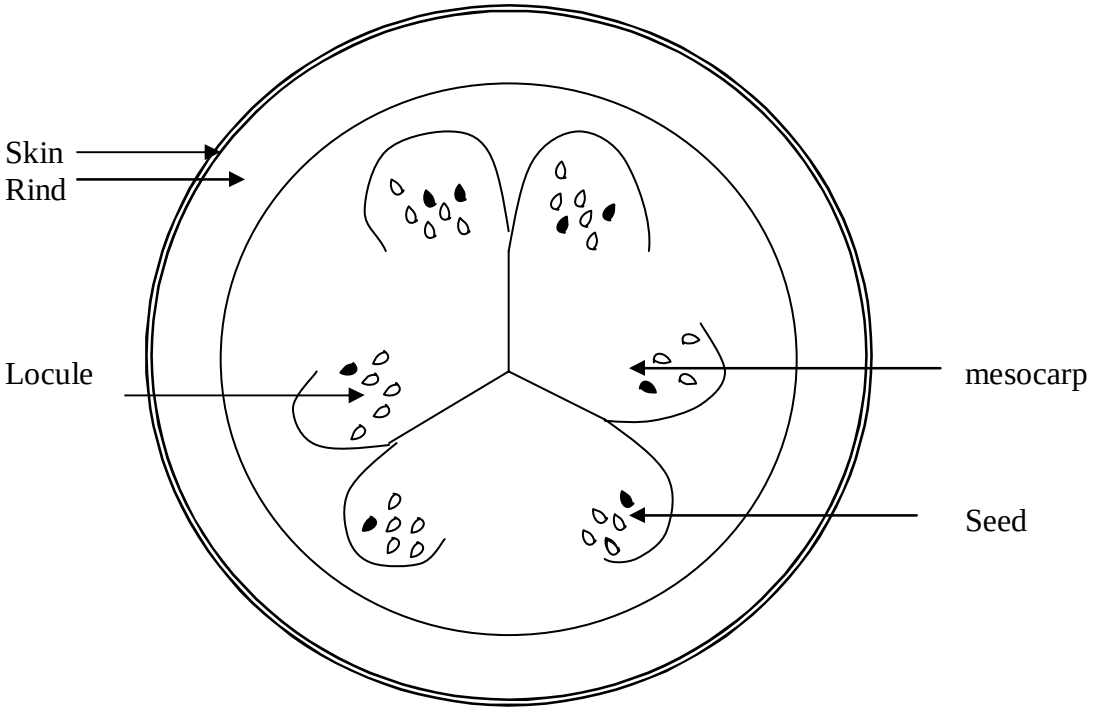


**Figure.2.4: Cross section of watermelon**

## 2.4 STABILITY OF LYCOPENE

Methods of lycopene assay should not destroy the lycopene. Therefore it is important to know the conditions under which lycopene containing products can be handled, processed and stored.

The lycopene in fresh tomato has 79-91% in the *trans* form whereas fresh watermelon juice contains about 94% *trans* lycopene (Collins, 2003). The degradation (instability) of lycopene occurs by isomerization and oxidation of *trans* lycopene. Though the bioavailability of *cis*-form is better than *trans* form (Boileau at al., 2002), the *cis*-

isomer is less stable because it is more prone to oxidation (Shi and Maguer, 2000). In watermelon, 50% of the lycopene is degraded during freeze-drying; whereas 20-40% loss occurs in freeze drying of tomatoes (Morningstar et al., 2003). Lycopene degradation was found to be more (6-15%) in cut watermelon than whole watermelon (6-10%), both stored at 13 and 5$^{o}$C, with no effect of temperature difference (Fish and Davis, 2003). During frozen storage of watermelon puree and chunk at –20 and –80$^{o}$C, Fish and Davis (2003) found that 30-40% loss occurred after a year, whereas only 5-10% occurred over the same period at –80$^{o}$C. The studies of stability of lycopene in tomato were mostly on the effect of heat processing and light (Shi and Le Maguer, 2000, Shi et al., 2003). Both heat and light caused degradation of lycopene in watermelon puree. However, lycopene was more stable in tomatoes during heating and illumination than lycopene in organic solvents (Shi and Le Maguer, 2000).

## 2.5 LYCOPENE ASSAY METHODS

Many methods have been developed for lycopene assay in tomatoes (Beerh and Sidappa, 1959; Adsule and Dan, 1979; Sadler et al., 1990; D'Souza et al., 1992; Arias et al., 2000). However, recently there have been some studies on lycopene assay in watermelon (Perkins-Veazie et al., 2001).

The current methods used to assay lycopene in fruits and vegetables are by extraction in organic solvents followed by spectrophotometric or chromatographic absorbance measurement at 503 nm. Both methods use organic solvents to extract and solubilize lycopene from tissues (Beerh and Sidappa, 1959; Adsule and Dan, 1979; Sadler et al., 1990).

Fish et al. (2002) developed a low volume hexane extraction method, which used 80% less organic solvents than the conventional spectrophotometric assay developed by Sadler et al. (1990). This method uses acetone, ethanol and hexane. A 0.6 g watermelon puree sample was taken and hexane was used to extract lycopene. The hexane layer was decanted and the absorbance value read at 503nm.

Arias et al. (2000) used an HPLC to measure lycopene concentration in tomatoes and tried to correlate the lycopene determined by HPLC to chromaticity values of the tomato surface measured with a portable Minolta chroma meter. The carotenoids were extracted from crushed and homogenized samples with a mixture of hexane, acetone and ethanol (50:25:25) while stirring for 15 minutes. Water was added and stirring was set for an additional 5 minutes to help the phase separation. The mixture was then filtered and the non-polar layers were separated from top layer by a syringe. The nonpolar phase was filtered with a 0.45 μm nylon filter and injected into the HPLC. The extraction method was performed under dark room conditions to avoid lycopene isomerization and degradation. A 4.6x250 mm, 5 μm, polymeric carotenoid $C_{30}$ column was used under the isocratic mobile phase of methyl alcohol and methyl tert-butyl ether in a ratio of 3:7. The lycopene standard used was 95% pure (Sigma Chemicals Co., St. Louis, MO) and showed a retention time of 9 minutes. The HPLC system consisted of a Waters 600E system controller (Millipore, Milford, MA) with a Waters 991 photodiode array detector. The wavelength range used was 420-530 nm and 471 nm was used to analyze the lycopene peak.

Ishida et al. (2001) developed an HPLC method for analysis of lycopene isomers from tomato. Reversed-phase HPLC (Waters model 2690, PAD 996, Millipore, Milford,

MA) with a $C_{30}$ column and a mobile phase consisting of methyl-t-butyl ether, methanol and ethyl acetate (40:50:10, v/v/v) was used. The system provided sharp resolution of lycopene isomers within approximately 23 minutes.

Although these chromatographic methods are reliable, they are laborious and require use and disposal of hazardous organic solvents. Skilled technicians are required to obtain reliable data using these complex instruments. An easy and reliable method to measure lycopene concentration that does not require hazardous chemical is needed for food and nutraceutical products.

D'Souza et al. (1992) related the concentration of lycopene with chromaticity values (from the CIE L*, a*, b* color model) of tomatoes. The lycopene concentration was calculated on the basis of the equation by Beerh and Siddappa (1959) after the sample absorbance had been read at 503 nm. Quantification of lycopene by spectrophotometric methods in the pericarp and of skin disk samples was performed. The best correlation that was found between lycopene and color was made with the $(a^*/b^*)^2$ factor. The relation between chromaticity and lycopene content was nonlinear.

Perkins-Veazie et al. (2001) tried to correlate tristimulus colorimeter readings (CIE L*, a*, b* values) from cut watermelons with lycopene content extracted from same melons. They did not find a correlation between tristimulus color and lycopene content of watermelon. They recommended the development of another method for quantifying lycopene without the use of organic solvents.

Davis et al. (2003a; 2003b) developed a method for assay for lycopene in watermelons and tomatoes using color absorbance of pureed samples. This method did not require any chemical reagent. They used a xenon flash colorimeter/spectrophotometer

and obtained absorbance spectra of watermelon puree at 400 to 700 nm. Absorbance at 700 nm was subtracted from absorbance at 560 nm for correlation with lycopene content. A good correlation was found between the absorbance difference (560 nm-700 nm) and lycopene content of watermelon and tomato puree determined by the low volume hexane extraction method.

The findings of Davis et al. (2003) were a very significant step towards elimination of the organic solvent procedure for estimation of lycopene content in watermelon and tomato. However this method still requires sample preparation steps of grinding watermelon flesh into puree, as well as use of an analytical laboratory spectrophotometer.

## 2.6 UV/VISIBLE SPECTROSCOPY AND OPTICAL PROPERTIES OF CAROTENOIDS

Out of the many analytical methods for compositional analysis of food and agricultural products, optical spectroscopy is a fast and nondestructive analytical tool. It does not alter or destroy the constituents of the products. Therefore it can be used for rapid sensing of food constituents online in a food processing plant or in the field. This section covers a brief theoretical background of UV/Visible spectroscopy, which will help in understanding the research.

Optical methods of chemical analysis rely on the interaction of electromagnetic radiation with matter. The wavelength range of radiation covered in optical spectroscopy can be divided into Ultraviolet (UV), 200 to 400 nm; and the visible, 400 to 760 nm. (Wolfbeis, 1991). When photons from UV and visible radiation interact with the electrons in molecular orbital of a matter, electrons from a low energy state in an orbital are promoted to a higher energy state (excited state). The shifting of electrons in discrete

energy levels is called electronic transition. In a molecule, the atoms can rotate and vibrate with respect to each other. These vibrations and rotations also have discrete energy levels, which can be considered as being packed on top of each electronic level. Because of the superposition of rotational and vibrational transitions on the electronic transitions, the UV/Visible spectra of a molecule have broad absorption bands. Thus a combination of overlapping lines (due to each electronic, vibration and rotational transition) appears as a continuous absorption band (Silberberg, 2000). Therefore, absorption bands of carotenoids have smooth and broad absorbance bands. Figure 2.5 shows the type of electronic transitions. Light absorption in carotenoids are due to excitation of electrons in π orbital to π* orbital (Britton, 1995a).

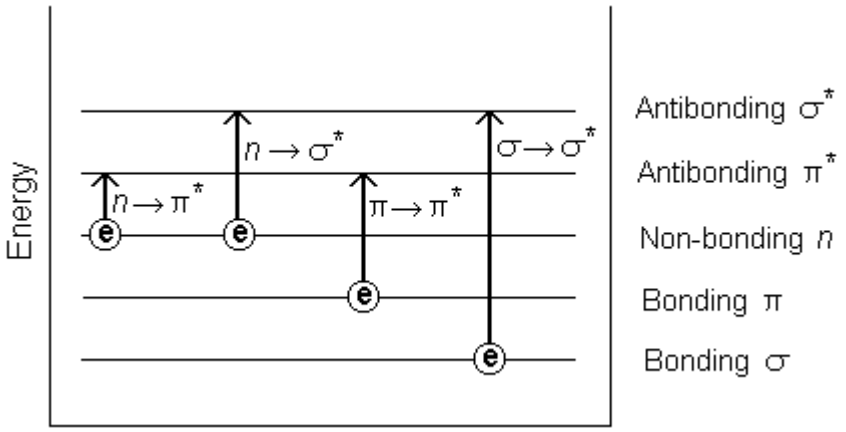


**Figure 2.5. Electronic energy levels and transitions (Anon 2004)**

The π electrons are highly delocalized and the excited state is of comparatively low energy, so the energy required to bring about the transition is relatively small and corresponds to light in visible region. Therefore the absorbance bands of the carotenoids are in the visible light region, and are responsible for their colors (Britton, 1995b).

### *2.6.1 Transmittance Spectroscopy*

UV/Visible transmittance spectroscopy is based on transmission of light through matter and selective absorption at specific wavelengths, based on the electronic transitions in the matter. As per the Beer Lambert law, if the radiation of a particular wavelength passed through a homogeneous solution in a cell, the intensity of the transmitted radiation reduces by an amount that depends upon the thickness and concentration of the material.

From figure 2.6, If $I_o$ is the intensity of the incident radiation and $I$ is the intensity of transmitted radiation, the ratio $I/I_o$ is called transmittance.

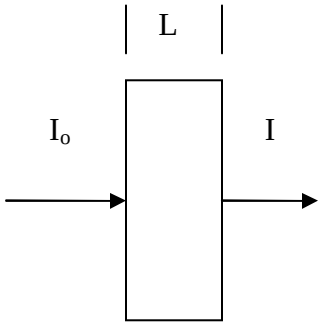


**Figure 2.6: Light transmission through a homogeneous material**

As per the Beer-Lambert law,

$$A = \log(I / I_o) = \varepsilon c L \qquad (2.1)$$

Where,

A = absorbance,

ε = extinction coefficient- depends on material and wavelength of the light,

c = concentration of absorbing molecules in path,

L = length of radiation path through the sample

The UV/Visible spectra of lycopene has three major absorption bands with absorption maxima at 446, 472 and 503 nm, with extinction coefficients, $\varepsilon_{max}$ = $1.206x10^5$, $1.850x10^5$ and $1.690x10^5$ $M^{-1}cm^{-1}$, respectively. These bands were observed when lycopene was dissolved in hexane (Mortan, 1975). Beta carotene has spectral bands at 430, 450 and 478 nm in hexane (Zang et al., 1997)

In conjugated polyenes like lycopene and other carotenoids, $\pi \rightarrow \pi^*$ transitions of energy levels occur upon absorption of light energy of a particular wavelength. Any charge around a molecule will alter the energy difference between ground state ($\pi$) and excited state ($\pi^*$). Therefore, an aqueous environment (being polar), reduces $\pi \rightarrow \pi^*$ transition energy due to a small decrease in energy of the $\pi^*$ orbitals, while the $\pi$ orbital energies remain unchanged. This results in less energy for $\pi \rightarrow \pi^*$ transitions. Thus a lower energy (longer wavelength) light can cause this transition, resulting in shift of absorbance band towards longer wavelengths in aqueous environment, called the red shift (Harris, 1996). Therefore, the absorbance peaks of lycopene and other carotenoids are red shifted in aqueous environments (such as in fruit tissues) as compared to the peaks of lycopene in hexane.

### *2.6.2 Diffuse reflectance spectroscopy*

Diffuse reflectance spectroscopy is a popular optical sensing technique and is the method by which we view most of our environment (Wolfbeis, 1991). The diffuse reflectance from a sample is obtained by penetration of a portion of incident light into the interior of the sample and partial absorption and multiple scattering in the sample (Wendlandt and Hecht, 1966). When light transmitted by a fiber optic probe is directed

into a turbid sample, light gets diffused due to absorption and scattering by particles. The diffuse reflectance measurement is valid for the diffusion area where sufficient multiple scatterings have taken place. The intermediate area between the source and the diffusion area is dominated by short-path, back-scattered, photons and the reflectance is not fully diffuse. The distance between the source and diffusion area depends on the scattering properties of the turbid sample (Crofcheck et al., 2002).

The most generally accepted theory concerning diffuse reflectance of materials composed of scattering and absorbing components is the Kubelka-Munk theory (Wendlandt and Hecht, 1966). For an infinite layer thickness (minimum thickness of material after which the reflectance is constant),

$$K/S = \frac{(1-R_\infty)^2}{2R_\infty} = F(R_\infty) \tag{2.2}$$

Where,

K = absorption coefficient

S = scattering coefficient

$R_\infty$ = reflectance at infinite layer thickness = $I/I_o$

$K = \varepsilon_R.c$, where $\varepsilon_R$ is comparable to molar absorption in the Beer-Lambert law.

Hence the relation between concentration c and Kubelka-Munk function $F(R_\infty)$ is given by

$$c = F(R_\infty)k' \tag{2.3}$$

Where $k' = S/\varepsilon$ is constant for a material. Hence the Kubelka-Munk function is proportional to the concentration of analyte and is analogous to the Beer Lambert law of transmission spectroscopy. Equation 2.3 is linear for scattering particles that are less than

1 mm in diameter. For larger particles and higher concentration, the plot of F ($R_\infty$) vs. concentration deviated from straight lines, by a decrease in slope at higher concentrations (Frei and MacNeil, 1973). However, for most practical applications, apparent absorbance values obtained by taking log of reflectance, $R_\infty$, are correlated with analyte concentrations (Hruschka, 2001)

## 2.7 FIBER OPTIC SENSORS

Optical fibers offer the advantage of transmitting light signals from sampling sites to remote locations and thus are flexible and convenient. For chemical sensing purposes, however, 1 to 100 m lengths of fibers are normally used (Wolfbeis, 1991). Optical fibers have potential for application in optical spectroscopy due to the availability of a wide range of light sources, detectors and amplifiers at low prices.

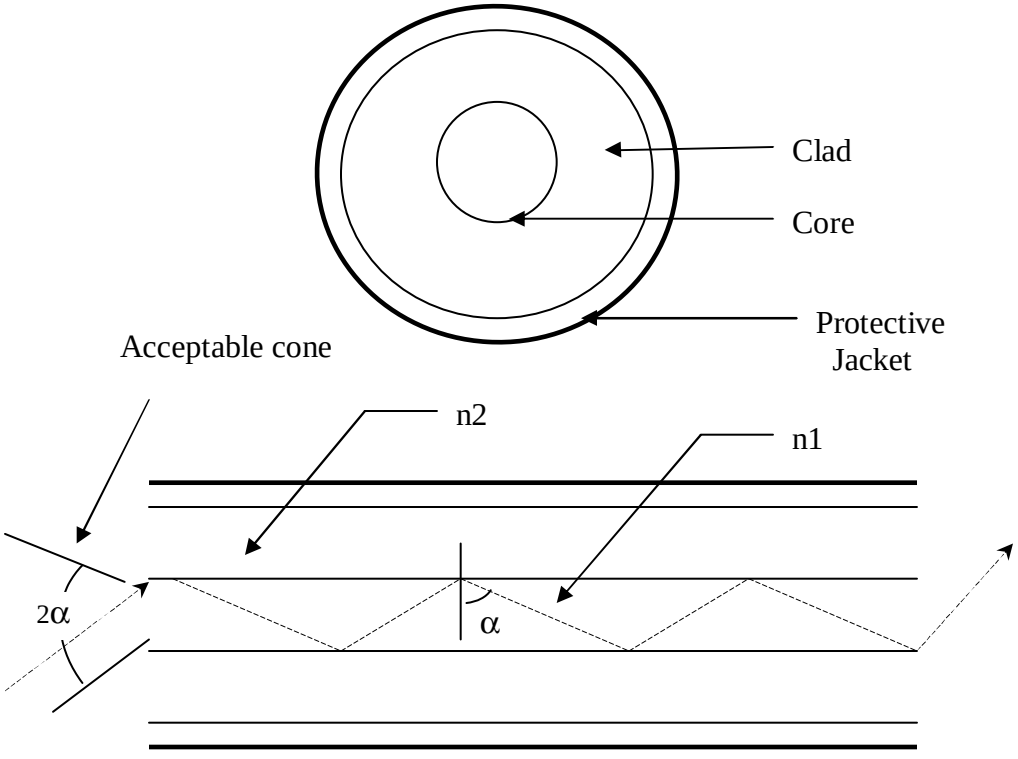


**Figure 2.7. Schematic of an optical fiber**

Optical fibers are based on the phenomena of total internal reflection. As shown in figure 2.7, step index fibers consist of a core of refractive index $n_1$, surrounded by cladding of lower refractive index $n_2$. Most fibers are covered with a protective jacket which has no effect on the waveguide properties.

If incident light strikes the fiber optic core at an angle greater than the critical angle, it is totally internally reflected at the interface of the core/cladding. Light entering the fiber within an acceptance cone (with apex half angle less than critical angle, $\alpha$) is transmitted. The acceptance cone half angle, $\alpha$, depends on the indices of refraction of core and clad as well as the refractive index of the outer medium, $n_o$ as presented in the equation below:

$$\sin \alpha = \frac{(n_1^2 - n_2^2)^{1/2}}{n_o} \qquad (2.4)$$

More commonly, the range of angles is described in terms of the numerical aperture (*na*), defined as:

$$na = n_o \sin \alpha \qquad (2.5)$$

Basically there are three types of optical fibers as listed below (Nolan et al., 1991):

1. Multimode step-index fibers
2. Multimode graded-index fibers
3. Single mode step-index fibers

Light propagates in discrete modes through a fiber. Each mode corresponds to a unique incident angle and has a distribution of electric and magnetic field vectors such that a given ray of light does not interfere with itself. The rays entering the fiber at

different angles travel different distances to reach to the end. This effect is called modal dispersion. The *na*, and thus modal dispersion, can be reduced by minimizing the difference between $n_1$ and $n_2$ and reducing the diameter of fiber. A single mode fiber has a diameter so small that (typically 3 to 5 μm) only a single mode can propagate.

Fiber optics can be used as intrinsic or extrinsic sensors. An intrinsic sensor utilizes the fact that any alteration in specific physical properties of the surrounding medium changes the light transmission characteristics of a fiber. In an extrinsic sensor, the fiber acts as a light guide. It allows remote spectrometric analysis of any analyte having an intrinsic optical property such as light absorption or emission that can be distinguished from the background. Extrinsic fiber optics can be used for spectroscopic sensing of lycopene in watermelon and tomato samples.

A fiber optic extrinsic sensor consists of a light source coupled to a fiber optic probe and a separate sample chamber. The transmitted or reflected light from the sample is usually received by another fiber and conveyed to a simple light detector or a spectrometer. For our research purposes, a fiber optic spectrometer was used to analyze reflected or transmitted spectra from watermelon and tomato samples.

## 2.8 MULTIVARIATE STATISTICAL ANALYSIS

Multivariate statistical techniques are powerful spectrum analysis tools for chemometry. Two commonly used multivariate regression techniques are; 1. Principal Component Regression (PCR); and 2. Partial Least Squares regression (PLS).

Before using these techniques, spectral data may be linearized by log transformation. Both of these regression techniques are based on data compression by projection of each spectrum (absorbance values in each wavelengths) onto an imaginary

axes called ‘principal components’, which account for most of the variations in the data. Each of the new variables, called ‘principal components’, are a linear combination of the original measurement along each wavelength, and contains information from the entire spectrum. The principal components obtained are regressed with analyte concentration in the PCR method. The PLS method creates new variables (principal components) by decomposing the original spectral data which are correlated and weighed proportionally with the analyte concentration. Thus PLS uses single step decomposition and regression. The first principal component (factor) captures maximum variation in the spectral data which are correlated to the concentration. The subsequent factors capture successively less variation in spectral data relevant to the concentration.

PLS regression has been extensively used for non-destructive quality evaluation of food and agricultural products by NIR spectroscopy (Williams and Norris, 2001; Lu and Ariana, 2002; Kawamura et al., 1999). PLS offers an advantage over PCR because the resulting spectral vectors are directly related to the constituents of interest, unlike PCR, where the vectors merely represent the most common spectral variations in the spectral data, completely ignoring their relation to the constituents of interest until the final regression step (Kramer, 1998).

# 3 MATERIALS AND METHODS

## 3.1 SAMPLES

Watermelons used for this study were grown at Oklahoma Vegetable Research Station, Bixby, Oklahoma in 2003 or were purchased from retail stores. Fruits grown at the research station at Bixby were the seedless cultivar 'Sugar Shack' and were under-mature (harvested 7-10 days prior to maturity) or mature. The origin and growing condition of purchased fruits were unknown. Tomatoes used for this study were purchased from local retail stores. The cultivars and post harvest history were not available for tomatoes.

In this study, transmittance and reflectance spectra were acquired from thin slices (2mm thick) and cubes ($2cm^3$) of watermelon flesh respectively. Thin slices were obtained using a meat slicer (Model 919/1, Berkel Inc., LaPorte, IN). Watermelon were cut by knife across the major axis, as shown in figure 3.1, and then placed on the feeder of the meat slicer to obtain round discs (slices) of watermelon. Watermelon slices of 2 mm thick were used as samples because thicker samples attenuated the light so much that there was very little signal to the spectrometer, and 2mm slice was the thinnest slice obtained from the available slicer.

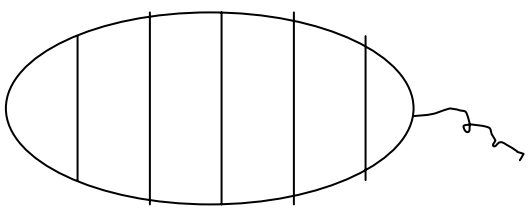

**Figure 3.1. Parallel lines show the direction of cut in the watermelon**

Samples of 2cm x 2cm rectangular thin slices were cut from these discs and used for transmittance measurements. Watermelon cubes of 2 cm sides were obtained by hand-cutting watermelon flesh by knife.

Reflectance spectra of watermelon and tomato puree were correlated with lycopene concentration. Watermelon flesh and whole tomato were pureed using an Omni mixer homogenizer (Omni Macro, Omni International Inc., Marietta, GA) to produce homogeneous slurry as per the sample preparation method suggested by Davis et al (2003b).

### 3.2 HARDWARE

A miniature fiber optic spectrometer (S2000 VIS-NIR, Ocean Optics, Inc., Dunedin, Fla.) was used for spectral measurements. The S2000 acquired spectra in wavelengths ranging from 350 to 1000 nm at 0.38 nm intervals. The S2000 had an optical resolution of 1.5 nm full width half maximum (FWHM). The spectrometer used a diffraction grating to separate incoming light into separate wavelength components. The separated light then fell onto a high-sensitivity linear Charge- Coupled Device detector (CCD, 2048-pixel Sony ILX511 linear sensor) through a 25-μm entrance slit. The CCD collected photons at each pixel during an integration time that was set by the operating software (OOI Base32, Version 2.0, Ocean Optics, Inc., Dunedin, Fla.). After the integration time was elapsed, the number of photons collected at each pixel location of the CCD (represented by a voltage) was transmitted from the CCD to an A/D converter board in the computer, where the voltage was converted to a 12-bit digital value. The data was displayed and

stored using the operating software OOI Base32 from Ocean Optics. A tungsten halogen light source (LS-1, Ocean Optics, Inc., Dunedin, Fla.) was used for this study.

### 3.3 Acquisition of Transmittance Spectra of Lycopene in Hexane

Transmittance spectra of standard lycopene (Sigma Chemical Co., St. Louis, MO) in hexane were obtained and compared with the literature values. The lycopene solutions in hexane were placed in the cuvette holder of an Integrated Sampling System (ISS-2, Ocean Optics, Inc. Dunedin, Fla.). It had a tungsten halogen light source with a diffuser on the illumination side and a collimating lens on the receiving side. A fiber optic cable (50 micrometer diameter, Ocean Optics, Inc., Dunedin, Fla.) was used on the receiving side for conveying the light transmitted through the sample to the S2000 spectrometer.

### 3.4 Acquisition of Transmittance Spectra from Watermelon Slices

A sample holder made of aluminum and coated with non-reflective black paint was used for obtaining light transmittance spectra through each watermelon slice. As shown in figure 3.2, it had a sample chamber, which had a slot in its bottom surface to hold a microscope glass slide. Thin slices of watermelon flesh were placed over the microscope slide to acquire their transmission spectra. Optical fiber of 400-micrometer diameter (P400-2-VIS-NIR, Ocean Optics Inc., Dunedin, Fla.) was used for conveying light from the light source and fitted to the upper side of the sample chamber with a collimating lens (74-ACR, Ocean Optics, Inc., Dunedin, Fla.). The light that was transmitted through the watermelon slice and microscope slide was received by the lower collimating lens of the sample chamber and conveyed to the spectrometer by a 50-micrometer diameter optical fiber (P50-2-UV-VIS, Ocean Optics, Inc., Dunedin, Fla.). An integration time of 100 mS

was used for transmission spectra collection while the integration time for the blank reference (transmittance of microscope glass) was taken at 5 mS.

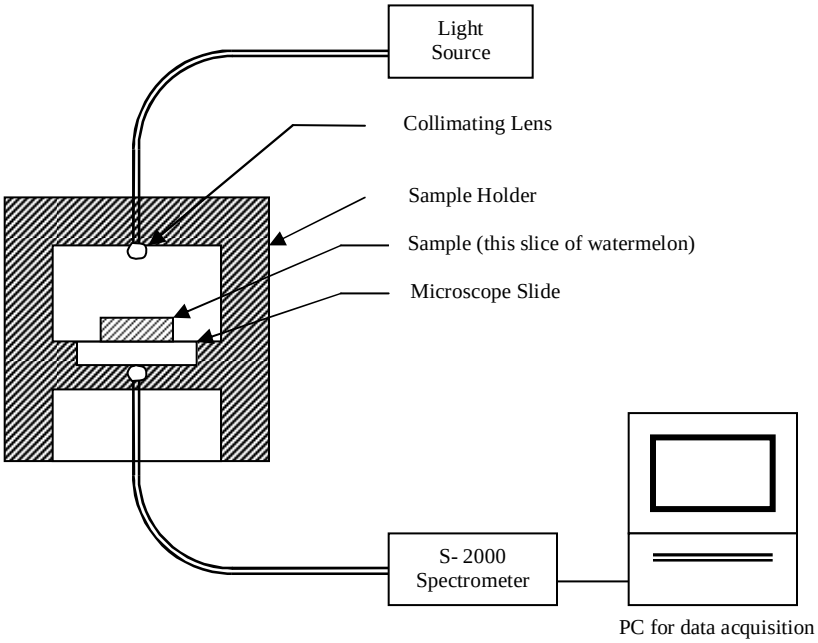


**Figure 3.2. Experimental setup for acquisition of transmittance spectra from thin slice of watermelon**

Therefore, absorbance values were obtained as follows:

$$A = \log\left(\frac{I_o/100}{I/5}\right) \qquad (3.1)$$

Where, A = absorbance in transmittance mode,

$I_o$ = intensity of light transmitted through the blank reference,

I = intensity of light transmitted through a watermelon slice.

The absorbance values were further analyzed as described in section 3.10.

### 3.5 ACQUISITION OF REFLECTANCE SPECTRA FROM WATERMELON CUBES

A bifurcated fiber optics of 200-micrometer diameter (BIF200-VIS-NIR, Ocean Optics, Inc., Dunedin, Fla.) was used for reflectance measurement. As shown in figure 3.3, one fiber was connected to a light source and the other to the spectrometer. The common end was used as probe for obtaining diffuse reflectance from samples. Two centimeter cubes of watermelon flesh, obtained from several locations of watermelon mesocarp, were used as samples and reflectance spectra were obtained from one face of each cube. All spectra were acquired under low ambient light level (approx. 34 $W/m^2$). A white diffuse reflectance standard (WS-1, Ocean Optics, Inc.) made of polytetrafluoroethylene (PTFE), a diffuse white plastic that provides a highly Lambertian surface, was used for taking reference spectra with an integration time of 5 mS. The bifurcated fiber optics probe was placed on the top of watermelon sample cube and three spectra of the surface were obtained. An integration time of 400 mS was used to obtain reflectance of samples; hence the actual reflectance values ($R_a$) were calculated as follows:

$$R_a = \left( \frac{I/400}{I_o/5} \right) = \left( \frac{R}{80} \right) \qquad (3.2)$$

Where, $R_a$ = actual reflectance,

I = intensity of light reflected from watermelon,

$I_o$ = intensity of light reflected from white reference,

R = reflectance = $I/I_o$

The reflectance data were linearized by taking log of $1/R_a$ (Hruschka, 2001) as shown in the equation below:

$$A_R = \log\left(\frac{1}{R_a}\right) \qquad (3.3)$$

Where, $A_R$ = apparent absorbance in reflectance mode.

Spectral data analysis were performed on the apparent absorbance values ($A_R$) as described in section 3.10

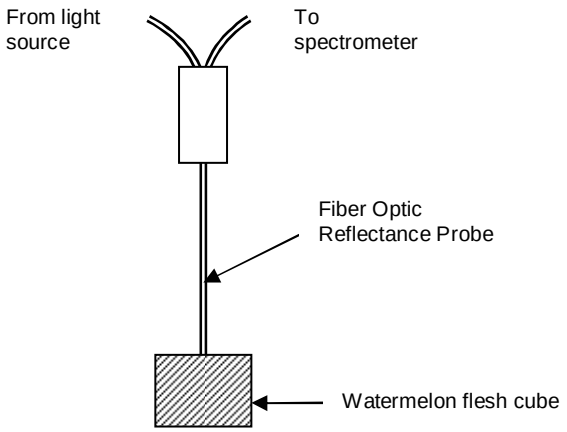


**Figure 3.3: Reflectance probe for obtaining reflectance spectra of watermelon flesh**

## 3.6 ACQUISITION OF REFLECTANCE SPECTRA FROM WATERMELON AND TOMATO PUREE

A bifurcated fiber optics (BIF200-VIS-NIR, Ocean Optics, Inc., Dunedin Fla.) was used as a reflectance probe, as explained in section 3.5. The reflectance probe was dipped in the pureed sample kept in 100 ml glass beaker at a depth of 1 inch between the tip of the probe and bottom of the beaker. Three spectra for each sample were obtained and averaged. Integration time of 300 mS was used for obtaining reflectance R, of samples. Reflectance data were linearized by taking the log of 1/R (Hruschka, 2001). Further data analyses were performed on these log (1/R) values, as described in section 3.10.

### 3.7 LYCOPENE ASSAY BY HEXANE EXTRACTION METHOD

The lycopene concentration was determined by the spectrophotometric procedure using hexane, acetone, ethanol and Butylated Hydroxytoluene (BHT) as described by the Sadler et al. (1990). After obtaining spectra of watermelon and tomato puree samples, 1mL puree sub samples were drawn in triplicate into preweighed amber-color 150mL glass bottles and weighed to obtain sample weight. Watermelon flesh samples were transferred to the brown bottles and weighed. A Sartorius balance with a 1mg resolution was used for weighing samples. One hundred mL hexane:acetone:ethanol (2:1:1 v/v/v) was added to each bottle. The bottles were closed and agitated for 10 min on a reciprocal shaker (Model 6010, Eberbach Corporation, Ann Arbor, MI) at 280 rpm and 1.5 inch stroke. This was followed by the addition of 15 mL of water and further shaking for 5 min. The bottles were then left at room temperature for 15 min to allow for phase separation. The mixed solution separated into a distinct aqueous polar layer (65 mL) and a nonpolar (50 mL) layer. A 4 ml aliquot from the top layer of nonpolar phase was carefully withdrawn using a glass pipette and filtered using Whatman® qualitative filter paper grade 1 (11 μm). The filtered hexane extract was taken in a 1-cm path length quartz cuvette and its absorbance relative to hexane was measured by a spectrophotometer (Shimadzu UV 160U, Shimadzu Scientific Instruments, Inc., Columbia. MD) at 503 nm. This wavelength was chosen to minimize any interference by any small amount of β-carotene present in the watermelon and tomato samples (Davis et al., 2003). Lycopene concentration in each sample was obtained by averaging the lycopene concentrations of triplicate sub-samples.

## 3.8 VARIABLE DISTANCE FIBER OPTIC PROBE

A fiber optic system was assembled for obtaining reflectance spectra of watermelon and tomato puree, at various distances between the light emitting and receiving fibers, as shown in figure 5.1. The fiber optic sensing system consisted of a linear translation stage (0.001 inch resolution, Ardel Kinamatic, Rochester, NY) with two stainless steel tubes (1 mm ID and 1.5mm OD) fitted in opposite sides of the stage so that they were aligned in parallel to each other and translated by turning the micrometer of the translation stage. Optical fibers of 1mm diameter (Super Eska, SH4001, Mitsubishi Rayon Co. Ltd, Tokyo, Japan) were inserted in the stainless steel tubes until the ends protruded through the tubes. The distance between the fiber optics inside the stainless steel tubes could be precisely varied using the micrometer of the translation stage to study the effect of center-to-center distance between fiber optics on the absorbance index. One of the fibers was connected to the tungsten halogen light source (LS-1, Ocean Optics, Inc., Dunedin, Fla.) and the other to the spectrometer (S2000 VIS-NIR, Ocean Optics Inc., Dunedin, Fla.).

## 3.9 ACQUISITION OF REFLECTANCE SPECTRA BY THE VARIABLE DISTANCE PROBE

All spectra were acquired under subdued light conditions at same level of illumination throughout the experiment. The white diffuse reflectance standard (WS-1, Ocean Optics, Inc., Dunedin, Fla.) was placed at 10 mm below the fiber optic probe and reference spectra at an integration time of 3000 mS were obtained. The reflectance values of the spectra of the white reference standard were converted to 100% values. The fiber optic probe was dipped in the pureed samples contained in brown bottles. Three spectra for each sample were obtained.

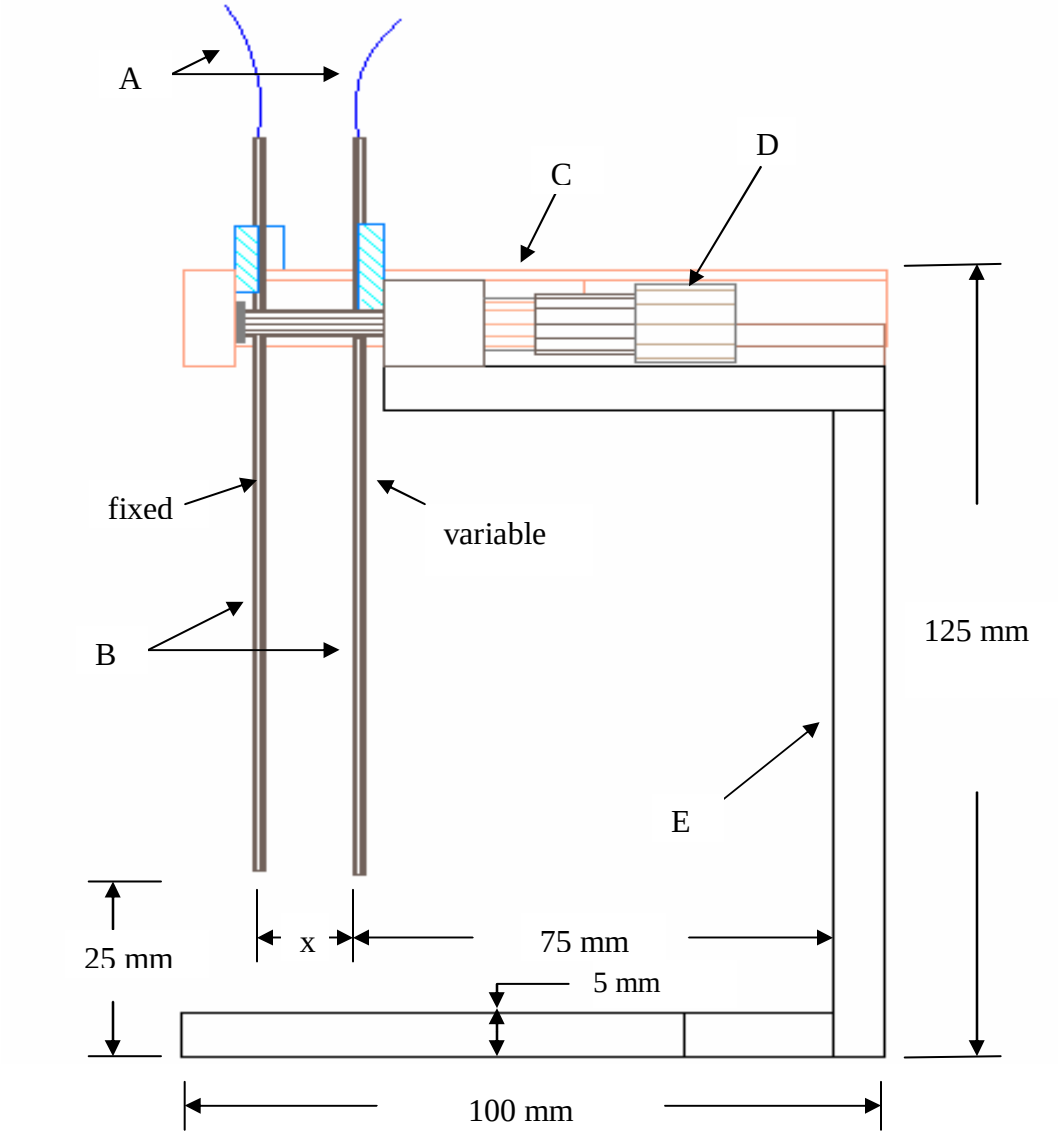


**Figure 3.4: Experimental arrangement for obtaining spectra of watermelon and tomato puree samples at variable distances between the light emitter and detector fiber optics.**

**A = light emitter and detector fiber optics of 1mm diameter.**

**B = stainless steel tubes of 1mm I.D. and 1.5 mm O.D.**

**C = translation stage.**

**D = micrometer screw for changing distance between fiber optics inside the stainless steel tubes.**

**E = support frame,**

**x = distance between optical fibers = 1.5 to 5.5 mm.**

An integration time of 3000 mS was used to obtain relative reflectance ratio R of samples. Reflectance data were linearized by taking log of 1/R (Hruschka, 2001). Further data analyses were performed on these apparent absorbance (Log (1/R)) values as described in section 3.10. The reflectance spectra of puree samples were acquired by fiber optics at successive increments of 0.5 mm distance between the fiber optics, starting from 1.5 mm and going to 5.5 mm.

## 3.10 SPECTRAL DATA ANALYSIS

The major peak of the spectral data was obtained at 565 nm. A baseline correction was applied by subtracting absorbance values at 700 nm according to the procedure established by Davis et al. (2003), as follows

$$AI = (A_{565} - A_{700}) \qquad (3.4)$$

Where AI is the absorbance index; $A_{565}$ is the absorbance at 565 nm and $A_{700}$ is the absorbance at 700 nm.

A Normalized Absorbance Index (NAI) was calculated to find a correlation between NAI and lycopene concentration using the following equation

$$NAI = \frac{(A_{565} - A_{700})}{(A_{565} + A_{700})} \qquad (3.5)$$

### *3.10.1 Least Squares Regression*

Least squares linear regression analysis of the AI and NAI to lycopene concentration was conducted. The linear regression model was used to predict lycopene concentration in validation samples. Coefficient of determination, standard error of prediction (SEP) and bias were used to evaluate the prediction ability of the models. SEP was obtained by

calculating standard deviation of residuals (difference between predicted and actual values of lycopene concentration). Mean values of the residuals were reported as bias.

### *3.10.2 PLS Regression*

Multivariate data analysis was performed with a commercial software package (Unscrambler® v7.8, Camo Process AS, Norway). Partial Least Squares type 1 (PLS1) Regression was used to develop calibration models correlating reflectance data with lycopene content for the wavelength region of 500 to 750 nm. The PLS algorithm extracts those factors (or principal components) from the entire range of spectra, which are most relevant for describing the response variables (lycopene concentration determined by hexane extraction). Hence this method is expected to give better correlation than the classical least squares regression. A full cross validation method was used for developing PLS1 models. The optimal number of factors (principal components) was determined by minimizing the predicted residual sum of squares (PRESS). The PLS models were evaluated by coefficient of determination, $R^2$, and standard errors of calibration (SEC) for the calibration sample set. The SEC for PLS regression model was calculated as follows

$$SEC = \sqrt{\frac{\sum_{i=1}^{n}(Y_{actual} - Y_{predicted})^2}{n - f - 1}} \qquad (3.6)$$

Where n = number of samples, f = number of principal components, $Y_{actual}$ = actual values of lycopene concentration, $Y_{predicted}$ = predicted lycopene concentration by the model.

Prediction ability of PLS models were evaluated by $R^2$, Standard error of prediction (SEP), and bias from the validation data set. SEP values were calculated as the standard

deviation of the residuals, as shown below and the bias values were obtained as the mean of the residuals.

$$SEP = \sqrt{\frac{\sum_{i=1}^{n}(Y_{actual} - Y_{predicted})^2}{n-1}} \qquad (3.7)$$

### *3.10.3 Statistical Analysis of Variable Distance Probe Data*

Reflectance spectra of watermelon and tomato puree acquired by the variable distance probe were analyzed to test the effect of lycopene concentration and distance between the source and detector fiber optics on Absorbance Index and Normalized Absorbance Index. The experimental data was analyzed as a factorial design with fruits as blocks. For each sample with a given level of lycopene concentration, the center-to-center distance between fiber optics was varied from 1.5 mm to 5.5 mm. Multiple regression models with absorbance index as a function of lycopene concentration and distance between fiber optics were obtained for watermelon and tomato puree, and the model coefficients were compared for their effect on the absorbance index.

# 4 RESULTS AND DISCUSSION

## 4.1 TRANSMITTANCE SPECTRA OF LYCOPENE IN HEXANE

A transmittance spectrum of lycopene in hexane acquired by the S2000 spectrometer is shown in figure 4.1. The absorbance peaks of lycopene spectrum were at 446 nm, 473 nm and 503 nm, and the maximum absorbance was at 472 nm. These absorbance peaks of lycopene match with the lycopene peaks reported in literature (Davies, 1976).

## 4.2 TRANSMITTANCE SPECTRA OF THIN SLICES OF WATERMELON FLESH

Figure 4.2 shows the absorbance spectra of watermelon slices. The major peak of lycopene in hexane at 503 nm was red-shifted to 565 nm. This red shift can be attributed to the highly polar aqueous environment around lycopene molecules in watermelon mesocarp cells. It was observed by Davis et al. (2003) at 560 nm in the spectra of watermelon puree. They used a xenon-flash spectrometer, which had a spectral resolution of 10 nm, and did not capture the actual peak at 565 nm, as observed by our high optical resolution (1.5 nm) spectrometer. The baselines of transmittance spectra for watermelon flesh samples were different due to the variation in sample constituents such as the fiber contents of the samples. The spectra in figure 4.2 were normalized and baseline corrected by calculating normalized absorbance values, NA, at each wavelength of spectra using the following equation:

$$NA = \frac{A_\lambda - A_{700}}{A_\lambda + A_{700}} \qquad (4.1)$$

Where, $A_\lambda$ = Absorbance at wavelength λ; $A_{700}$ = absorbance at 700 nm.

The normalized spectra are presented in figure 4.3.

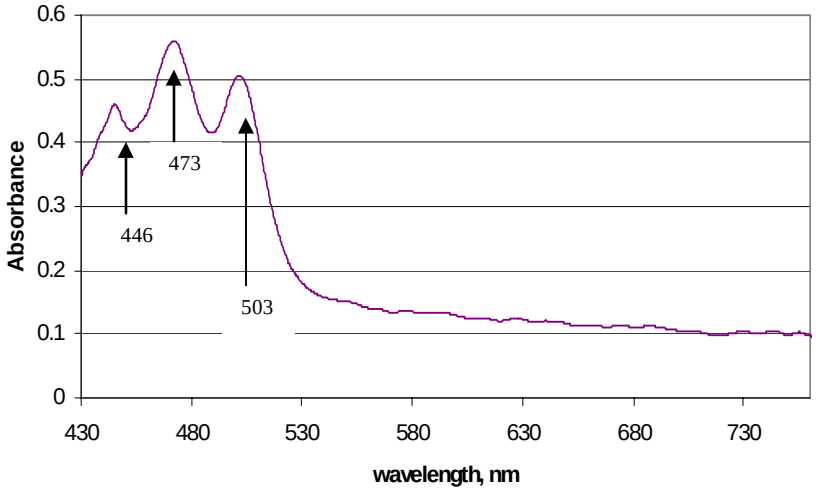


**Figure 4.1. Transmittance spectra of lycopene solutions in hexane**

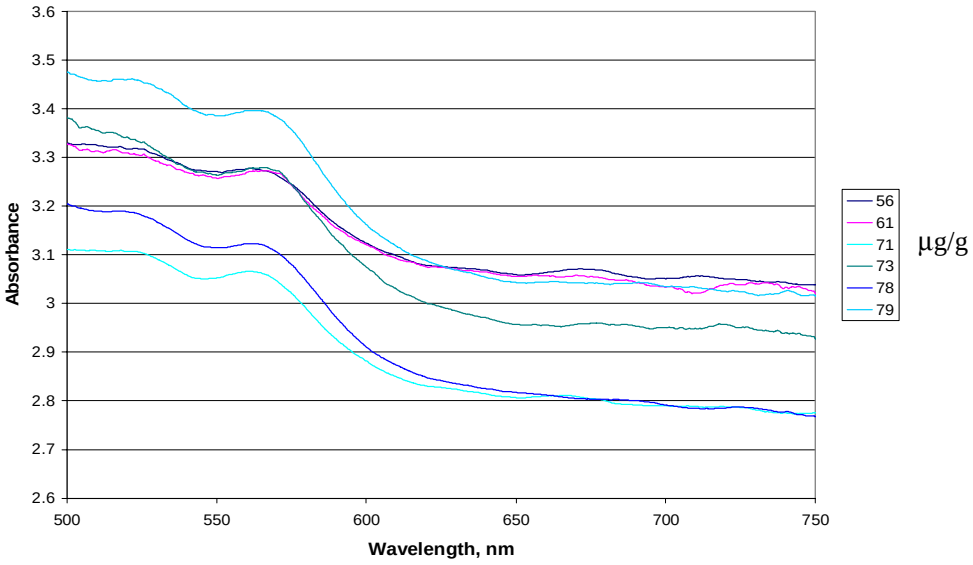


**Figure 4.2. Transmittance spectra of 2mm thick watermelon slice samples at various lycopene concentrations, µg/g**

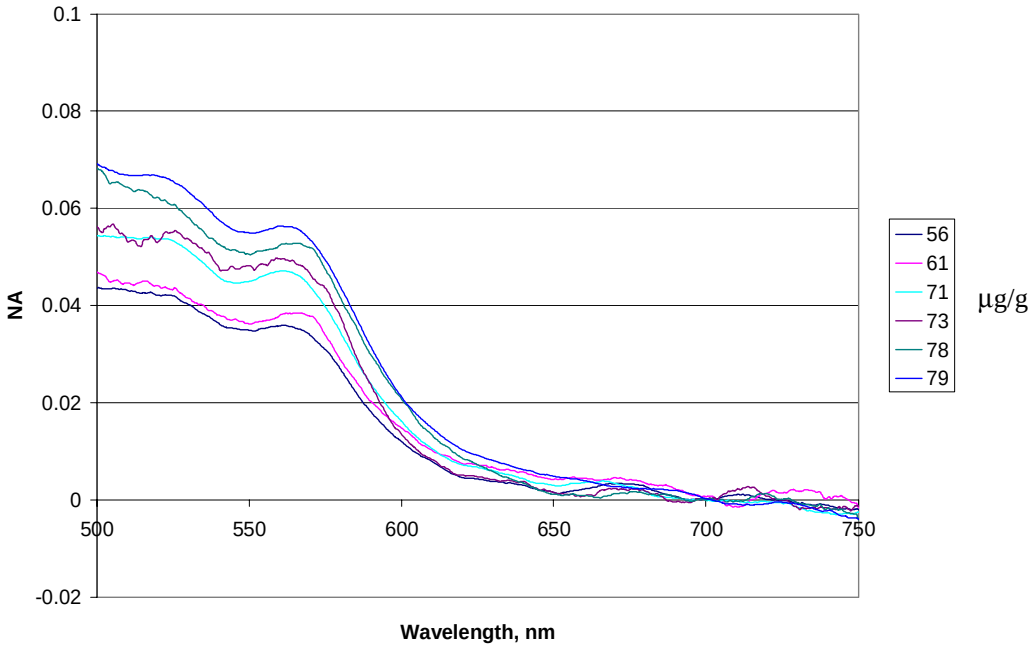


**Figure 4.3. Normalized transmittance spectra of 2mm thick watermelon slice samples at various lycopene concentrations, µg/g**

## 4.3 LEAST SQUARES REGRESSION FOR TRANSMITTANCE SPECTRA FROM THIN SLICES OF WATERMELON

Figure 4.4 shows the least squares regression of absorbance-index (AI) and normalized absorbance index (NAI) of 60 watermelon slice samples with lycopene concentration. Descriptive statistics of the watermelon slice samples are presented in table 4.1. The lycopene concentration of the calibration sample set varied from 46.5 to 89.9 µg/g, with a mean and a standard deviation of 72.0 and 10.9 µg/g, respectively. From figure 4.4 and table 4.2, the $R^2$ values for the AI and NAI regression were 0.67, and 0.66 respectively. The standard error of calibration for AI regression model was 6.1 µg/g, whereas that for NAI was 6.4 µg/g. The LS regression models for AI and NAI gave higher error than the hexane extraction method which had an error of ± 3.0 µg/g. The

overall error in lycopene concentration measurement by hexane extraction method was calculated by error analysis of the individual measurements involved in hexane extraction method. The calculation of overall error in hexane extraction procedure was presented in appendix A.

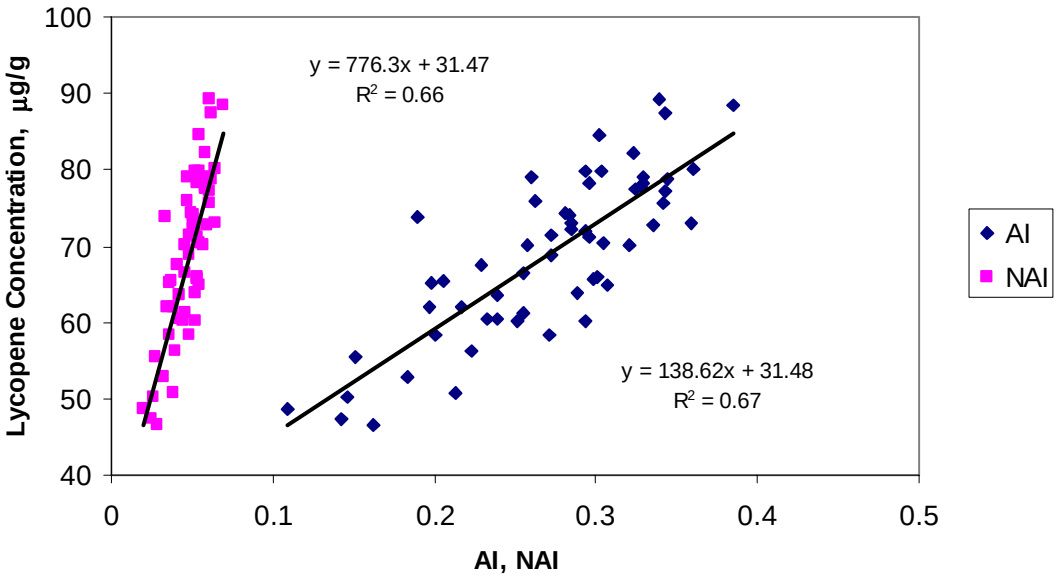


**Figure 4.4. Correlation of Absorbance Index (AI) and Normalized Absorbance Index (NAI) with lycopene concentration of thin slices of watermelon**

**Table 4.1: Descriptive statistics of watermelon sample used for calibration and validation of LS and PLS regression models**

| Sample set | | No. of samples | Lycopene Concentration (µg/g) | | |
|---|---|---|---|---|---|
| | | | Mean | S.D. | Range |
| Thin slices | calibration | 60 | 72.0 | 10.9 | 46.5 - 89.9 |
| | validation | 60 | 72.0 | 10.9 | 46.5 - 89.9 |
| Cubes | calibration | 40 | 54.1 | 19.2 | 19.9 - 87.4 |
| | validation | 20 | 58.0 | 21.6 | 23.2 - 89.2 |

## 4.4 PLS REGRESSION FOR TRANSMITTANCE SPECTRA FROM THIN SLICES OF WATERMELON

To improve the correlation between spectral data and the reference method, multivariate method of regression, namely, PLS was tried on the absorbance spectra. Prior to regression, spectra were normalized and mean centered. The PLS method calculated principal components which were linear combinations of the absorbance values (independent variable), that described most of the variations in the response variable. This model had potential to give better correlation because it extracted the features from the entire spectrum.

The Partial Least Squares (PLS) regression with cross validation was used for the spectral range of 500 to 750 nm for the same set of samples as used for the Least Squares (LS) correlation. A plot of calibration and validation data points is shown in figure 4.5. The PLS results are also summarized in table 4.2.

**Table 4.2: Summary of results from watermelon flesh calibration models**

| Sample | Spectra mode and Regression | $R^2$ of calibration | SEC (μg/g) | SEP (μg/g) |
|---|---|---|---|---|
| 2 mm thick Slice | Transmittance, LS | 0.67 | 6.1 | - |
| | Transmittance, PLS | 0.62 | 6.7 | 7.5 |
| *2 cm cubes* | Reflectance, PLS | 0.94 | 4.9 | 5.2 |

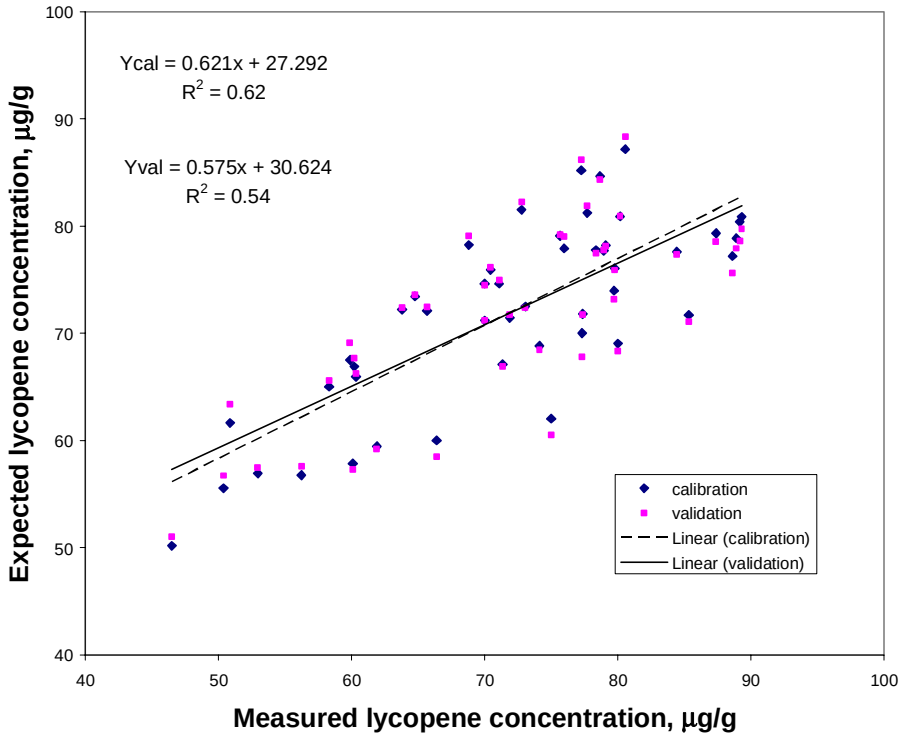


**Figure 4.5. Results of PLS regression on transmittance data from thin slices of watermelon**

The $R^2$ values for calibration and validation were 0.62 and 0.53 respectively. The standard errors of calibration and cross validation were 6.7 and 7.5 µg/g respectively. Hence the PLS model did not predict better than the least square regression models. Because of high attenuation of light by watermelon flesh, a good prediction model could not be obtained from the transmittance spectra of watermelon slice. Therefore, a reflectance spectra method for watermelon flesh was explored.

## 4.5 REFLECTANCE SPECTRA OF WATERMELON FLESH CUBES

The second derivative reflectance spectra of the apparent absorbance (log $(1/R_\infty)$) from watermelon flesh samples (2 cm cubes) are shown in figure 4.6. The second derivatives of the spectra had taller peaks and were normalized and baseline corrected as

a result of the derivative. The most prominent absorbance maxima peak at 565nm were transformed to minima values (valleys) by the second derivative transformation. The next prominent absorbance maxima were at 760nm. These peaks are the absorbance peaks of water, as reported in literature (Buiteveld et al., 1994). Since this peak was not related to the lycopene concentration, it was not included in the regression analysis.

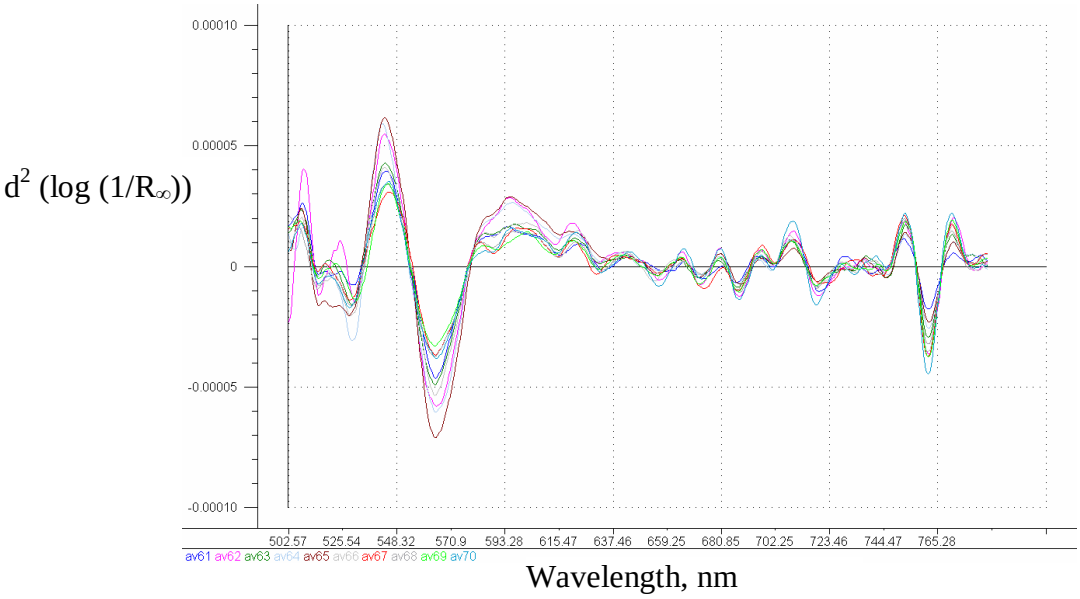


**Figure 4.6. Second derivative spectra of log (1/R∞) from ten samples of watermelon flesh**

## 4.6 PLS REGRESSION OF REFLECTANCE SPECTRA FROM WATERMELON FLESH CUBES

A PLS model was developed and validated from 60 watermelon cube samples in the wavelength range of 500 to 750 nm. Two thirds of the samples (40 samples) were randomly assigned as a calibration set and the rest (one third or 20 samples) were assigned as a validation set. Descriptive statistics of the samples used for reflectance spectra calibration and validation are presented in table 4.1. The mean and standard

deviation of the calibration sample set were 54.1 and 19.2 µg/g respectively with range of 19.9 to 87.4 µg/g. The validation samples had a mean and standard deviation of 58.0 and 21.6 µg/g respectively and ranged from 23.2 to 89.2 µg/g. Three factors (principal components) could explain 100% of the variation in the independent variables (absorbance values) and 93% of the variation in the dependent variable (lycopene concentration measured by hexane extraction method).

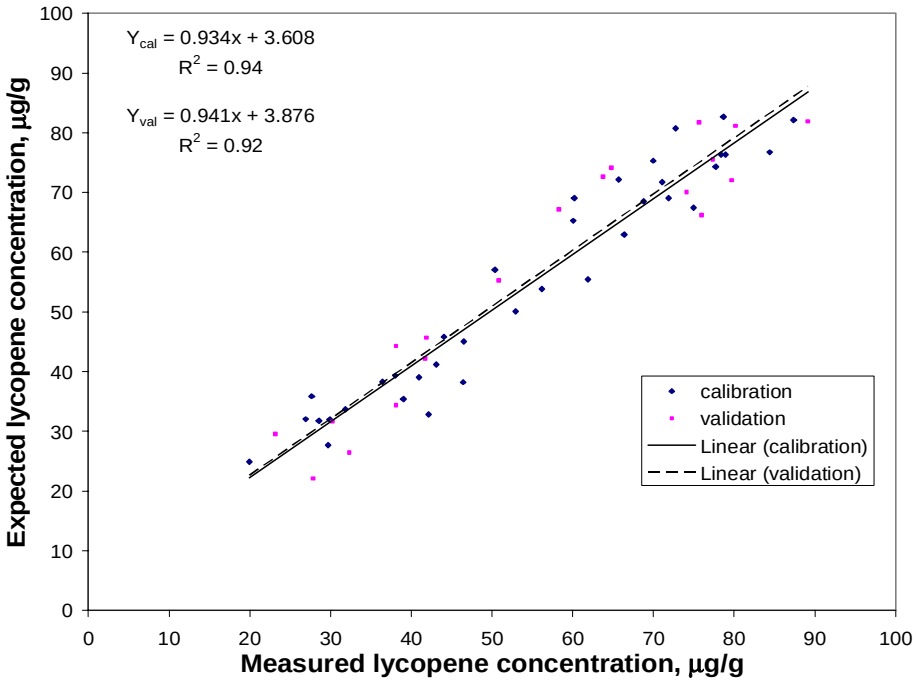


**Figure 4.7. Measured versus predicted lycopene concentration by PLS1 model developed from reflectance spectra on watermelon flesh**

Figure 4.7 shows the measured versus predicted regression lines for the calibration and validation sample sets. From figure 4.7 and table 4.2, the $R^2$ value for calibration was 0.94 and that for validation was 0.92. The standard errors of calibration and prediction were 4.9 and 5.2 µg/g respectively. We can expect this model to predict lycopene

concentrations in 95% of the samples to within an error limit of ±5.2 μg/g. This error is higher than the overall error of lycopene measurement by the hexane extraction method (± 3.0 μg/g). The error may be due to the small area of view of the fiber optics reflectance probe (200 μm diameter fibers with $25^{o}$ field of view). The PLS model of the reflectance spectra of watermelon flesh can be used as a basis for classifying watermelons based on their lycopene concentrations such as 'low' (30 μg/g or lower), 'medium' (40 to 60 μg/g), and 'high' (70 μg/g or higher) lycopene watermelons.

## 4.7 CONCLUSIONS FROM WATERMELON FLESH STUDY

The Absorbance Indexes (AI) obtained from transmittance spectra (by subtracting absorbance at 700nm from the peak absorbance at 565 nm) of watermelon slices were linearly correlated ($R^2 = 0.67$) with the lycopene concentration measured by hexane extraction. This is significant information for the design of an optical sensor to estimate lycopene concentration in watermelon flesh. The Normalized Absorbance Index (NAI) was also linearly correlated with lycopene concentration, but it had a slightly lower $R^2$ value (0.66) than the AI correlation. The high attenuation of light caused by scattering effects of fibers and other constituents of watermelon flesh gave a low transmittance signal in the transmission mode. Therefore, reflectance spectra from watermelon flesh were acquired and used for development of a multivariate PLS regression model. The PLS model from reflectance spectra had $R^2$ values of 0.94 and 0.92 for calibration and validation respectively, with SEC of 4.9 μg/g and SEP of 5.2 μg/g. This model can be used as a basis for a rapid estimation technology of lycopene in watermelon flesh and for classification of watermelons into low, medium, and high lycopene categories.

## 4.8 REFLECTANCE SPECTRA OF WATERMELON AND TOMATO PUREE

The reflectance spectra and normalized reflectance spectra of watermelon puree are shown in figures 4.8 and 4.9 respectively. The major peaks of lycopene spectra in hexane at 503 nm were red shifted to 565 nm as observed in the transmittance and reflectance spectra of watermelon flesh in figures 4.2, 4.3 and 4.6.

Comparing spectra of watermelon and tomato purees from figures 4.8 and 4.10, the average apparent absorbance values (log $(1/R_a)$) for watermelon puree was higher than the tomato puree. This may be due to the higher concentration of particulates in tomato puree samples as compared to watermelon puree samples. The mean path length of the light into the sample material decreases with decreasing size and increasing concentration of particulates, allowing less interaction between light and material, causing lower absorption of light (Dahm and Dahm, 2001). Absorbance values at individual wavelengths depend on many factors including lycopene, particle size and concentration, refractive index of the particles and surrounding medium of sample materials, intensity of light, and the distance between the light source and detector fiber optics (Dahm and Dahm, 2001, Meeten and Wood, 1993).

The normalized spectra of watermelon and tomato puree samples are shown in figures 4.9 and 4.11 respectively. By normalizing, the baseline shifts in the spectra of individual samples were removed and peak heights at 565 nm were adjusted such that the peaks at 565 nm gave the values of NAI.

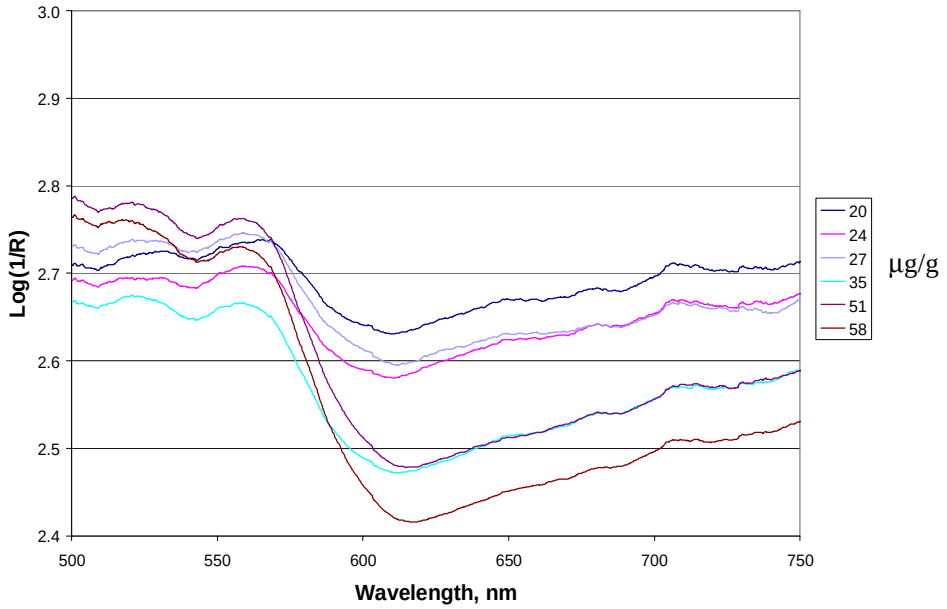


**Figure 4.8. Reflectance spectra of watermelon puree samples with different lycopene concentrations, µg/g**

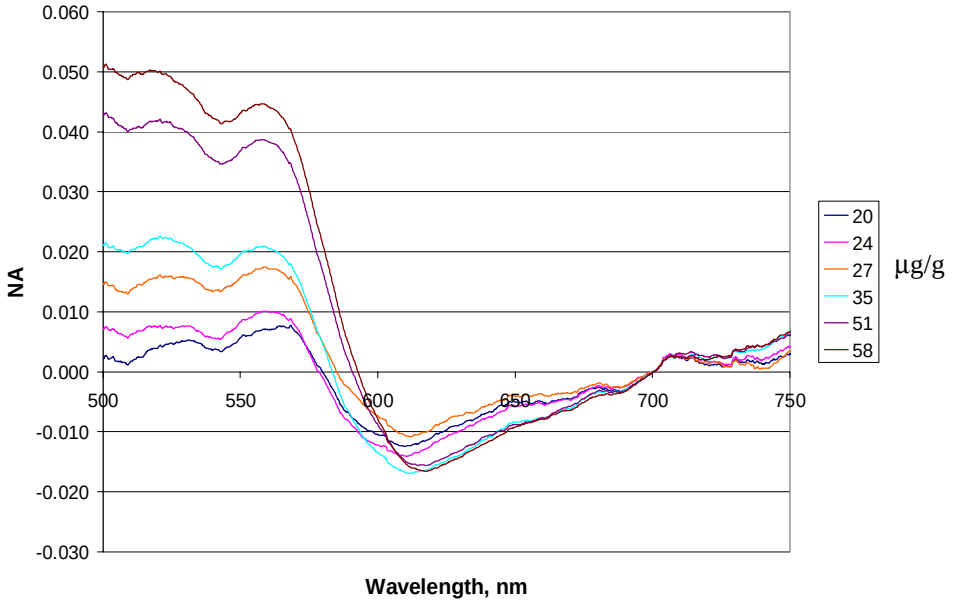


**Figure 4.9. Normalized reflectance spectra of watermelon puree samples with different lycopene concentrations, µg/g**

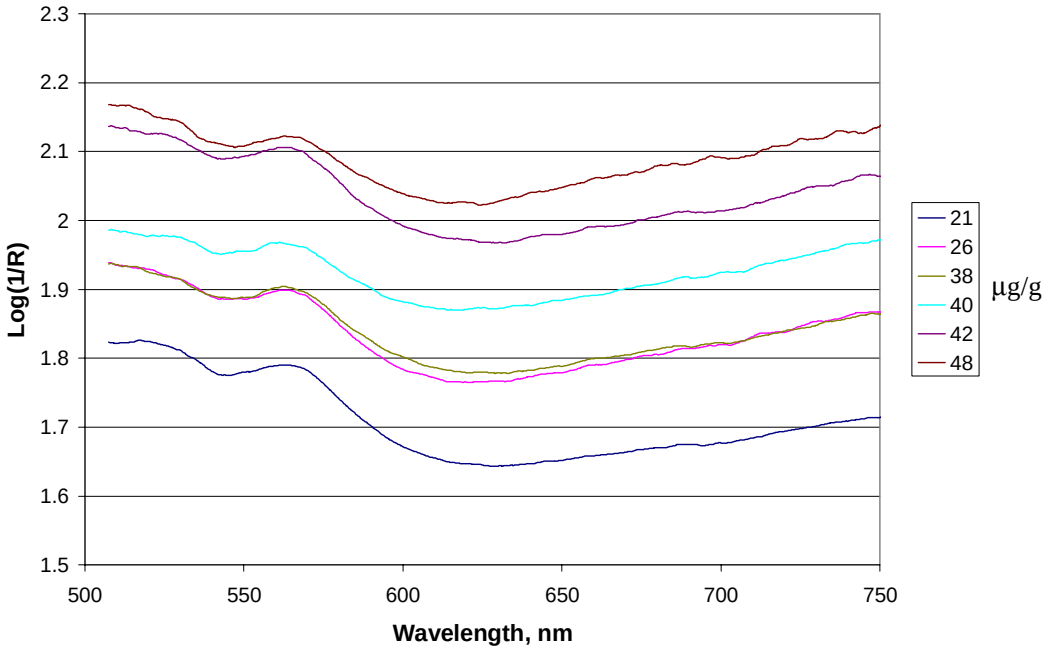


**Figure 4.10. Reflectance spectra of tomato puree samples with various lycopene concentrations, µg/g**

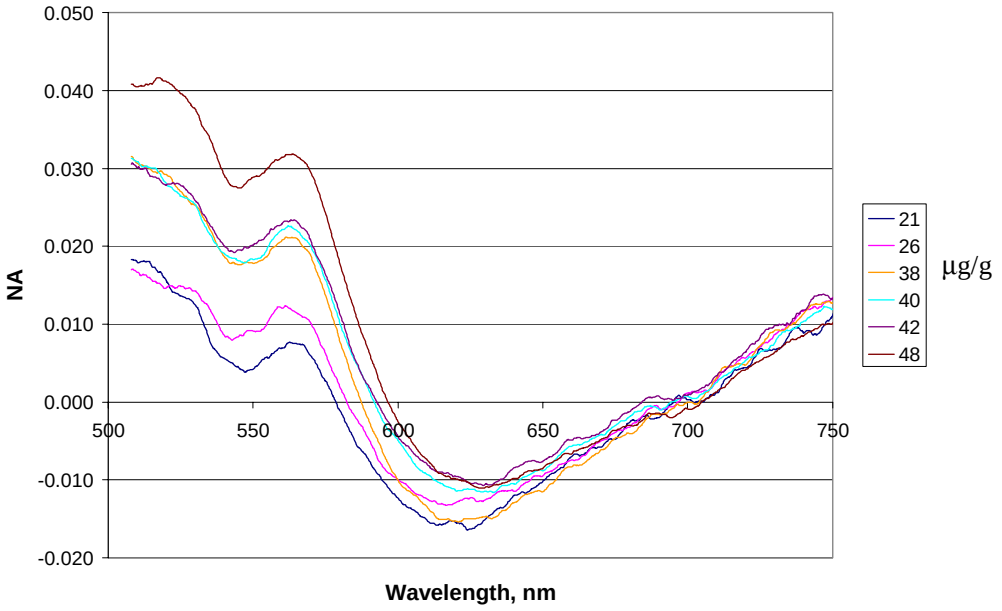


**Figure 4.11. Normalized reflectance spectra of tomato puree samples with various lycopene concentrations, µg/g**

## 4.9 REGRESSION OF WATERMELON AND TOMATO PUREE REFLECTANCE

### *4.9.1 Sample Statistics*

Total of 110 samples were used for development and validation of regression models for each fruit. Table 4.3 shows the descriptive statistics for the samples used for calibration and validation of regression models. Lycopene concentrations in 70 samples of the calibration set for watermelon puree varied from 19.9 to 80.7 μg/g and that in 40 samples of the validation set varied from 19.3 to 79.0 μg/g. For tomato puree, 67 samples were used for calibration with a lycopene concentration ranging from 10.0 to 50.5 μg/g and 43 samples were used for validation with a lycopene concentration of 15.4 to 42.9 μg/g.

**Table 4.3: Summary of sample sets used for calibration and validation of lycopene concentration in watermelon and tomato puree**

| Sample set | | No. of samples | Lycopene concentration of samples, μg/g | | |
|---|---|---|---|---|---|
| | | | Mean | S.D. | Range |
| Watermelon puree | Calibration | 70 | 49.9 | 15.4 | 19.9 - 80.7 |
| | Validation | 40 | 42.9 | 18.7 | 19.3 - 79.0 |
| Tomato puree | Calibration | 67 | 25.6 | 10.9 | 10.0 - 50.5 |
| | Validation | 43 | 27.8 | 6.7 | 15.4 - 42.9 |

### *4.9.2 LS Regression of Watermelon Puree Reflectance*

Absorbance Index (AI) and Normalized Absorbance Index (NAI) from reflectance spectra of watermelon and tomato puree were correlated with lycopene concentration. As

shown in figure 4.12, both the AI and NAI had a high linear correlation with lycopene concentration of watermelon puree ($R^2$ = 0.90 for both AI and NAI). The slope of the least squares model for NAI increased due to normalization. The LS models developed for watermelon and tomato purees are shown in table 4.4. For AI models, the regression coefficient (slope of the linear model) for tomato puree was higher than that of watermelon puree. Therefore, the model for watermelon puree was less sensitive to the absorbance index than the tomato puree model. However, when the spectra were normalized, the slopes of NAI models for both fruits increased and came closer to each other such that there was no significant difference between them (P=0.0941). However, there was a significant difference between the intercepts (P<0.0001).

Figure 4.13 shows the measured and predicted values of lycopene concentrations in calibration and validation sample sets of watermelon puree. A summary of calibration and validation statistics for watermelon and tomato puree samples is presented in table 4.5. The LS linear regression model for watermelon puree as shown in table 4.5 and figure 4.13 could predict lycopene concentration in validation samples with $R^2$ =0.93, SEP = 5.1 μg/g and bias = 2.1 μg/g.

**Table 4.4: Least squares linear regression models developed for watermelon and tomato puree**

| Sample set | Regressor | Model | $R^2$ |
|---|---|---|---|
| Watermelon puree | AI | Y = 144.36x + 14.48 | 0.90 |
| | NAI | Y = 786.66x + 15.262 | 0.90 |
| Tomato puree | AI | Y =202.66x + 21.42 | 0.78 |
| | NAI | Y = 780.36x+21.54 | 0.61 |

Y = lycopene concentration, μg/g, x = AI or NAI

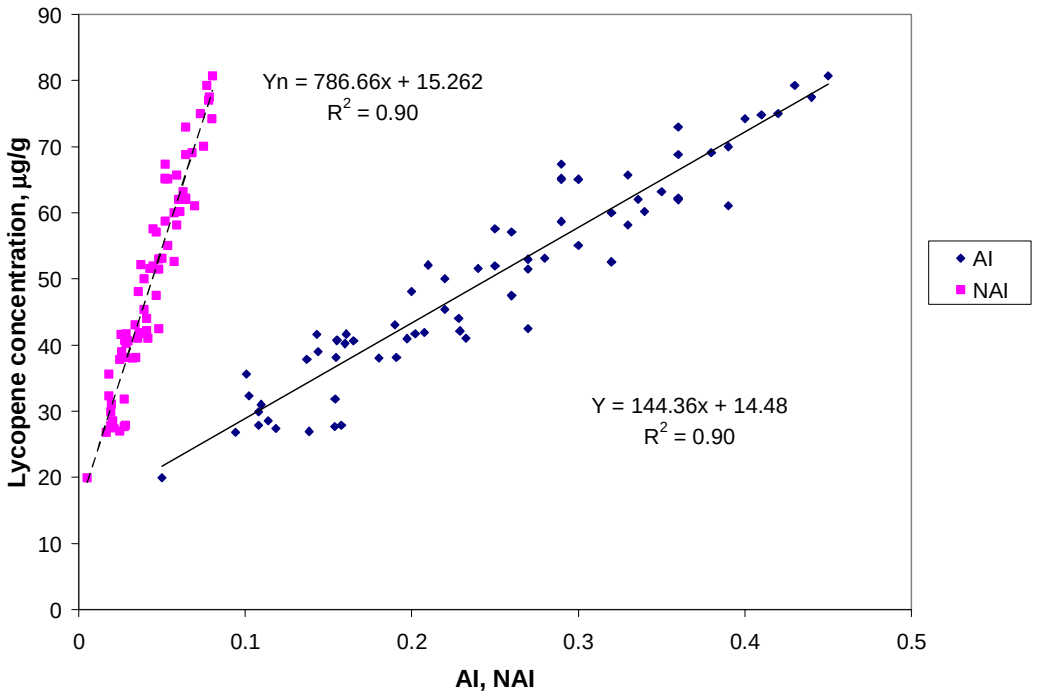


**Figure 4.12. Correlation of Absorbance Index and Normalized Absorbance Index with lycopene concentration of watermelon puree**

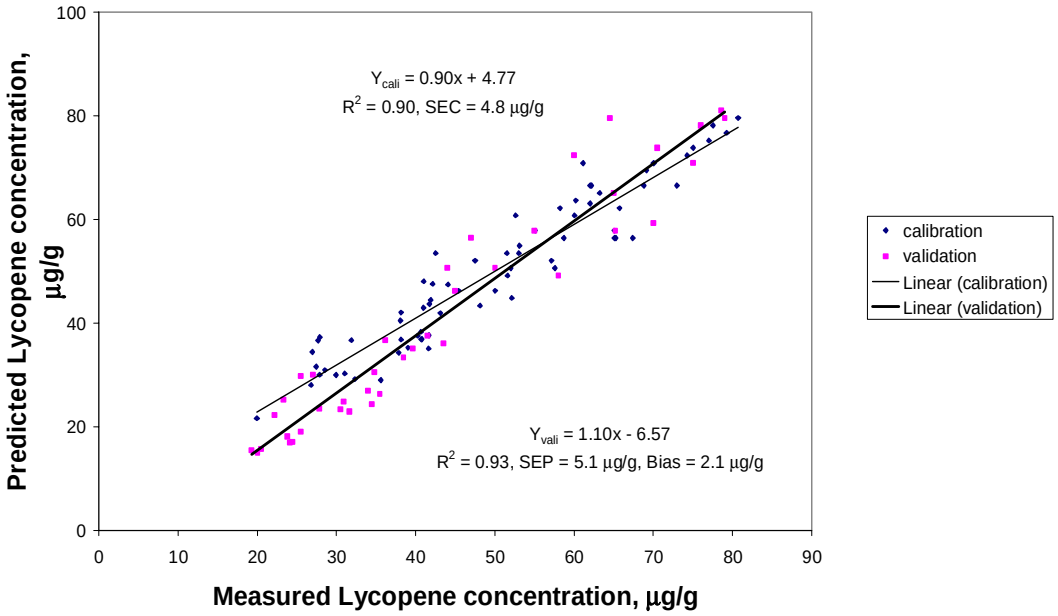


**Figure 4.13. Least Squares regression and prediction for watermelon puree samples**

**Table 4.5: Summary of calibration and validation statistics for watermelon and tomato puree samples**

| Sample set | Model | Calibration | | | Validation | | |
|---|---|---|---|---|---|---|---|
| | | Factors | $R^2$ | SEC (μg/g) | $R^2$ | SEP (μg/g) | Bias (μg/g) |
| Watermelon puree | LS | 1 | 0 .90 | 4.8 | 0.93 | 5.1 | 2.1 |
| | PLS | 3 | 0.97 | 2.4 | 0.97 | 3.4 | 0.0 |
| Tomato puree | LS | 1 | 0.62 | 6.7 | 0.54 | 5.2 | -3.3 |
| | PLS | 3 | 0.93 | 2.9 | 0.88 | 2.5 | 0.5 |

### *4.9.3 PLS Regression for Watermelon Puree Reflectance*

A PLS regression model was developed for watermelon puree using all the wavelengths in the spectrum range of 500 to 750 nm. The performance of the PLS model for watermelon puree is summarized in table 4.5 and a plot of actual and predicted values of lycopene concentration of samples is presented in figure 4.14. The PLS model predicted lycopene concentrations in validation samples with an $R^2$ value of 0.97, and a SEP of 3.4 μg/g, without bias. Compared to the least squares model, the PLS model had a better prediction ability with less error. This may be possible because the PLS algorithm has the capability to capture the relevant significant variance in the independent variables in the first few important principal components (factors) and send the noise values to the later factors (Williams and Norris, 2001).

The prediction error of the PLS model for watermelon puree was nearly equal to the precision of the hexane extraction method (±3.0 μg/g). Davis et al. (2003a) developed

a least squares linear regression model by correlating absorbance index (absorbance at 560nm – absorbance at 700 nm) of watermelon puree with lycopene concentration. They reported that the least squares model had similar precision as the hexane extraction method.

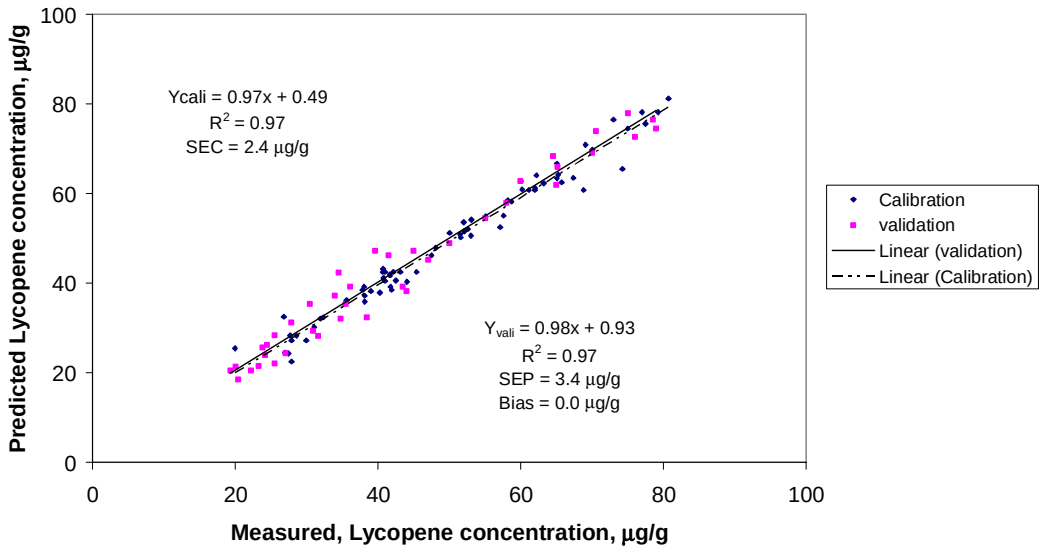


**Figure 4.14. Performance of watermelon puree PLS regression model with 3 PC**

They used a xenon flash spectrophotometer with an integrating sphere sensor, which was bulky and therefore non portable. The fiber optic method tested in this study could have practical application for on-site or online sensing of lycopene concentration in liquid product lines requiring continuous monitoring of lycopene concentration for quality assurance. Being miniature in size and having capability of transmitting light over long distance, a fiber optic reflectance probe can easily be installed in process equipment compared to existing technology.

The least squares model from watermelon puree had better correlation with a higher $R^2$ value of 0.93 as compared to $R^2$ of 0.72 of the least squares model developed from reflectance spectra of watermelon flesh samples. This may be due to the improved homogeneity of pureed samples of watermelon compared to intact watermelon flesh.

### *4.9.4 LS Regression of Tomato Puree Reflectance*

The least squares regression of the absorbance index of tomato puree samples with their lycopene concentration had an $R^2$ value of 0.62 as presented in figure 4.15. Notice the negative values of absorbance index for tomato puree samples with lower lycopene concentration. Significantly high correlation of absorbance index with lycopene concentration in the case of tomato puree indicates that the absorbance index can be used to predict lycopene concentration in tomato puree irrespective of the sign of the absorbance index. The negative absorbance index could be due to higher scattering of light at 700 nm caused by higher particulate concentration, and lower absorbance at 565 nm due to the comparatively lower lycopene concentration of tomato puree samples. The NAI had an $R^2$ value of 0.61, which was slightly less than the AI model. Hence the AI model was used for validation.

Referring to table 4.5 and figure 4.16, the least squares model for tomato puree predicted lycopene concentration in tomato puree validation samples with an $R^2$ value of 0.54, SEP of 5.2 µg/g and bias of -3.3 µg/g. Davis et al. (2003b), used a xenon flash spectrophotometer in transmittance mode to correlate scatter adjusted absorbance at 560nm (absorbance at 560nm – absorbance at 700nm) with lycopene concentration in tomato puree. They obtained an $R^2$ value of 0.96 by using only 13 tomato samples for

developing a least squares model, but did not validate it, and the performance of their model is unknown.

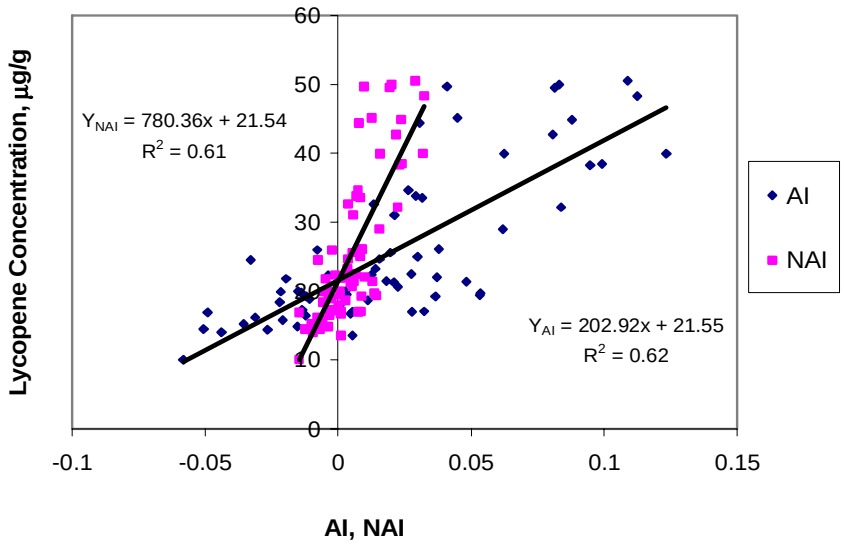


**Figure 4.15. Correlation of Absorbance Index (AI) and Normalized Absorbance Index (NAI) with lycopene concentration of tomato puree**

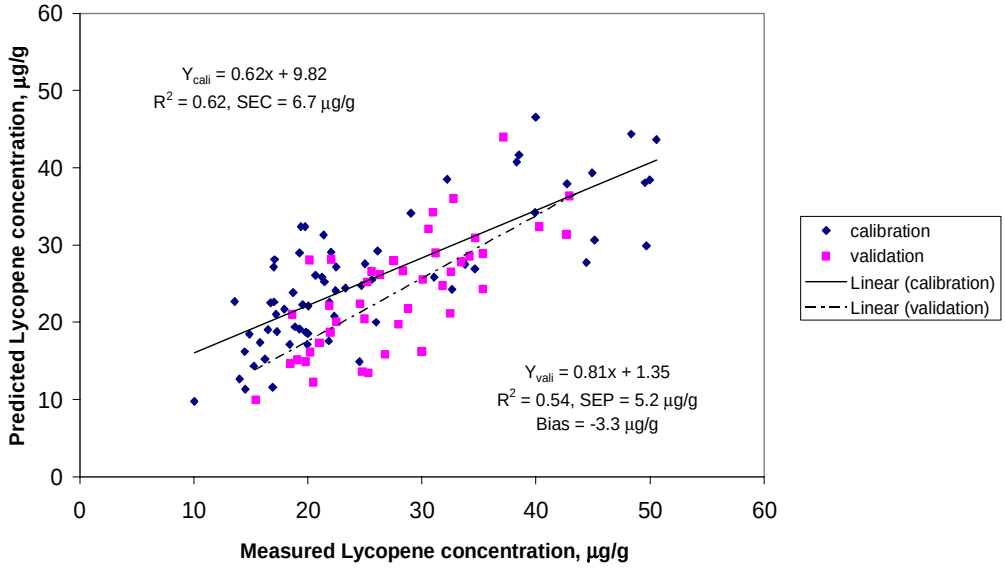


**Figure 4.16. Least squares regression and prediction of lycopene concentration in tomato puree**

### *4.9.5 PLS regression of Tomato Puree Reflectance*

A PLS model was developed using all values of absorbance (log ($1/R_a$)) from reflectance spectra of tomato puree in the wavelength range of 500 to 700nm. A comparison of calibration and validation samples is presented in figure 4.17. As summarized in table 4.5, the PLS model with 3 principal components, had better predictive ability than the least squares model. The PLS model predicted lycopene concentration in validation samples of tomato puree with an $R^2$ value of 0.88, an SEP of 2.5 µg/g and a bias of 0.5 µg/g, which was better than the least squares regression model.

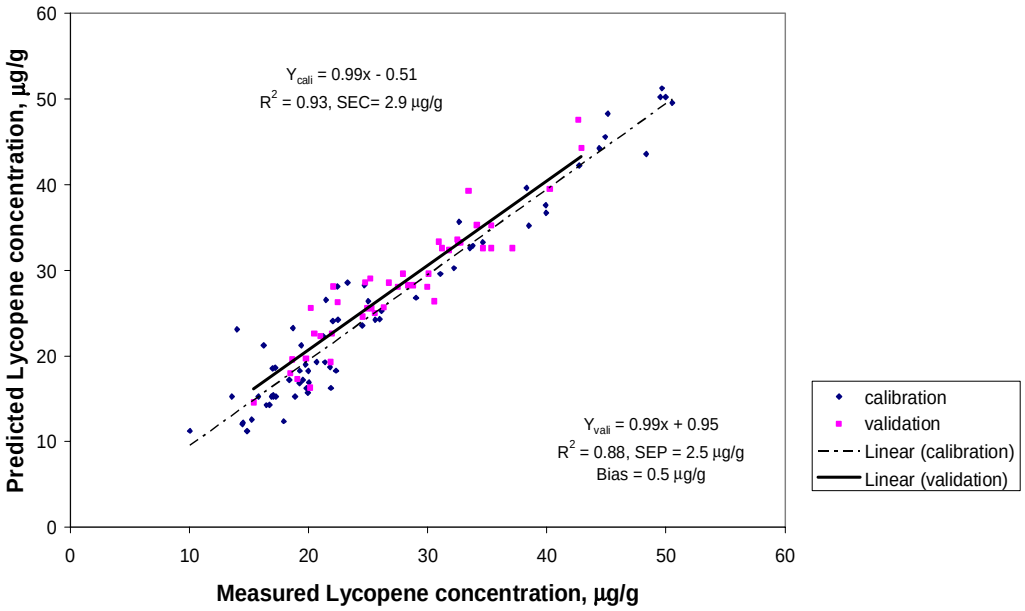


**Figure 4.17. Performance of PLS regression model of tomato puree samples with 3 principal components**

## 4.10 CONCLUSIONS FROM REGRESSION ANALYSIS OF PUREE REFLECTANCE

The absorbance index and normalized absorbance index obtained from absorbance values at 565 nm and 700 nm from reflectance spectra of watermelon and tomato puree were linearly correlated with the lycopene concentration of watermelon and tomato puree

samples ($R^2$ = 0.90 for watermelon and 0.62 for tomato). This is very important information for the design of a fiber optic reflectance sensor for estimating lycopene concentration of watermelon and tomato puree, as two monochromatic light sources of 565 nm and 700nm could be used for lycopene sensing. The PLS models, developed by a cross validation method using all absorbance values from reflectance spectra in the wavelength range of 500-750 nm, performed very well during validation with separate validation sample sets. The PLS model for watermelon puree could predict lycopene concentrations in validation samples with an $R^2$ value of 0.97, an SEP of 3.4 μg/g. The PLS model for tomato puree performed well by predicting lycopene concentration in validation samples with an $R^2$ value of 0.88, an SEP of 2.5 μg/g and a bias of 0.5 μg/g.

Thus the fiber optic reflectance probe can be used reliably for rapid quantification of lycopene in watermelon and tomato puree samples. It has the advantage of being rapid, as it does not require any further sample preparation of watermelon and tomato puree. Fiber optic sensing of lycopene does not destroy the pureed samples. This method has a high practical significance for online sensing of lycopene concentration in product lines requiring continuous monitoring of lycopene concentration. Moreover, utilizing miniature light sources and photo detectors, a portable fiber optic lycopene sensor could be designed for use in the field, laboratory, or processing plant.

### 4.11 SPECTRA OF WATERMELON AND TOMATO PUREE BY 1MM FIBER OPTIC PROBE

The visible spectra of watermelon puree acquired by the 1 mm diameter variable distance probe (fig. 3.3) were compared with the spectra obtained by the 200 micron bifurcated fiber optics (fig. 4.18). The average apparent absorbance values (Log (1/R)) for watermelon puree samples increased with an increase in distance between the emitter

and detector fiber optics. This indicated that the loss of light intensity, due to absorbance and scattering, increased proportionally with the distance between the light source and the detector due to the interaction of light with the thicker sample layer.

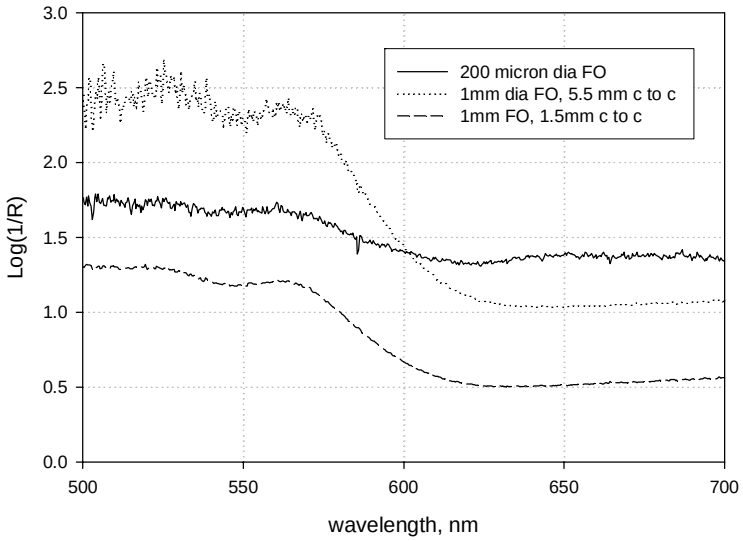


**Figure 4.18. Comparison of reflectance spectra of watermelon puree acquired by 1 mm fiber optic probe with two separation distances, and a 200 mm bifurcated fiber optics. The lycopene concentration of watermelon puree was 50.6 μg/g.**

For bifurcated fiber optics, the average absorbance values above 600 nm were higher than the 1 mm fiber optic probe system. This baseline shift could be due to the lower intensity of light delivered by the 200 micron fiber (approx. 135 $W/m^2$) as compared to the 1 mm fiber (approx. 1,170 $W/m^2$). The spectra in figure 4.18 were normalized using equation 4.1 and presented in figure 4.19. The NA values of normalized spectra from the variable distance probe at different separation distances were closer to each other than the NA values of the spectrum by the 200 micron probe. This might be due to the higher intensity of light conveyed to the sample by the 1 mm diameter probe than the 200 micron probe.

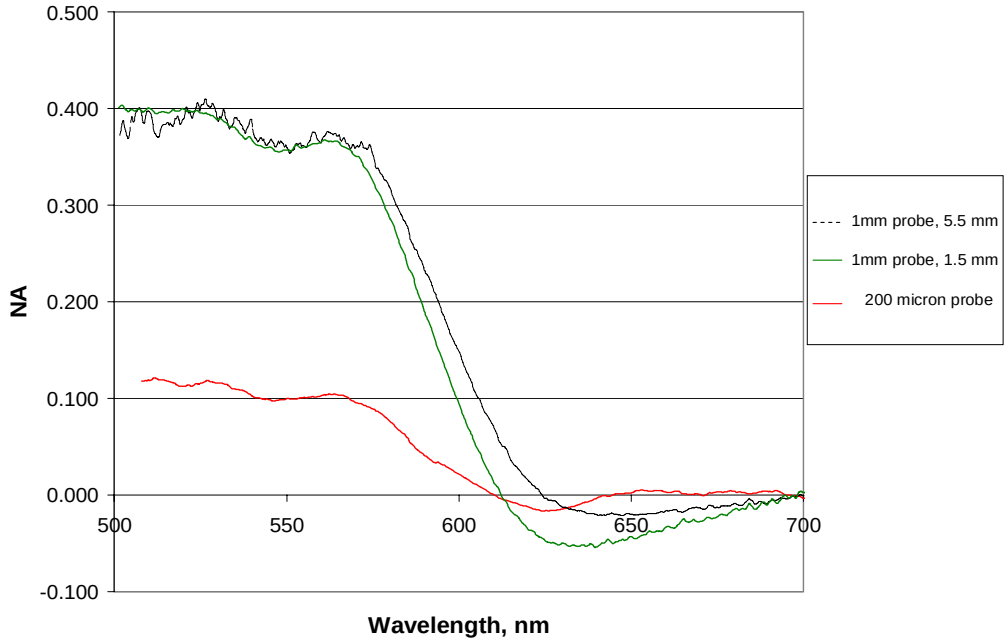


**Figure 4.19. Comparison of normalized reflectance spectra of watermelon puree acquired by 1 mm fiber optic probe with two separation distances, and a 200 mm bifurcated fiber optics. The lycopene concentration of watermelon puree was 50.6 µg/g**

Figure 4.20 shows the comparison of spectra of tomato puree at four levels of lycopene concentrations and two levels of center-to-center distances between 1mm fiber optics. The peak heights of the sample spectra increased with lycopene concentration and distance between the emitter and detector fiber optics. The baseline of the spectrum also increased with increasing center-to-center distance between the fiber optics, due to increased sample thickness between the light source and detector fiber optics. The spectra in figure 4.20 were normalized and presented in figure 4.21. The absorbance values of spectra with different fiber optic distances came closer to each other and thus the effect of distance was reduced in the normalized spectra, which was also observed in case of watermelon puree spectra in figure 4.19.

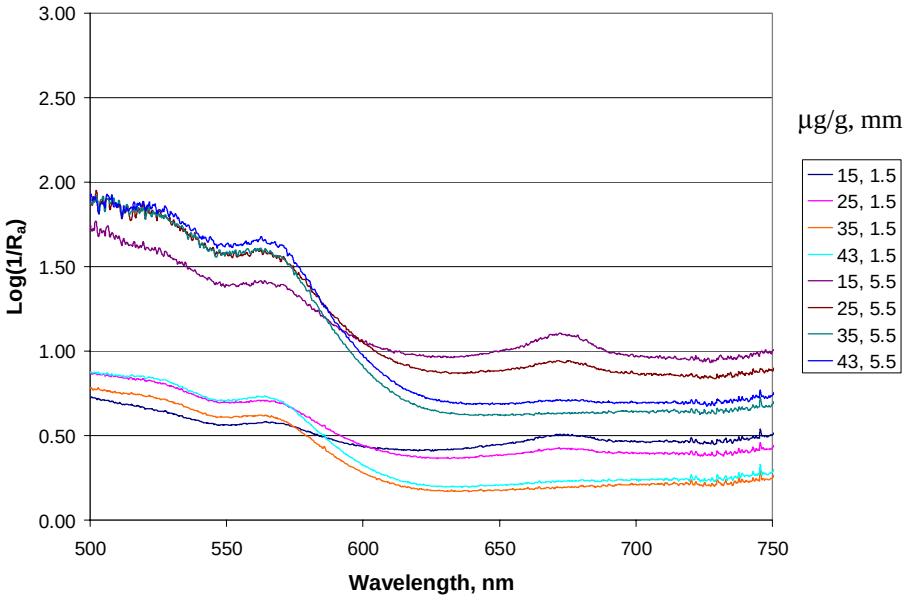


**Figure 4.20. Comparison of reflectance spectra of tomato puree acquired by 1 mm fiber optics probe with minimum (1.5mm) and maximum (5.5mm) center-to-center distance between emitter and detector fiber optics at various lycopene concentration in µg/g.**

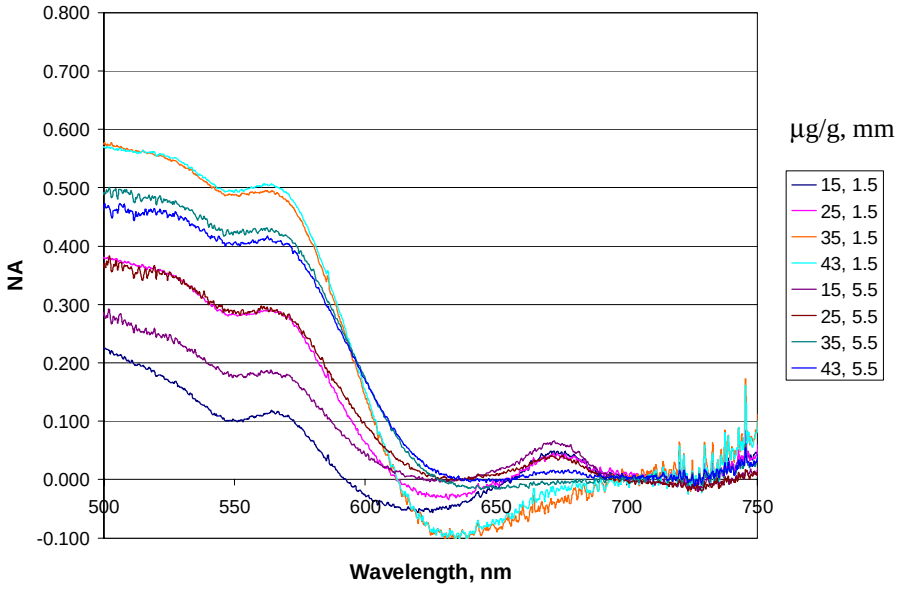


**Figure 4.21. Comparison of normalized reflectance spectra of tomato puree acquired by 1 mm fiber optics probe with minimum (1.5mm) and maximum (5.5mm) center-to-center distance between emitter and detector fiber optics at various lycopene concentration in µg/g.**

## 4.12 EFFECT OF FIBER OPTIC DISTANCE AND LYCOPENE CONCENTRATION ON AI AND NAI

Table 4.6 shows the descriptive statistics of the watermelon and tomato puree samples used for this study. For watermelon, 21 samples were used with lycopene concentration varying from 11.2 to 57.7 μg/g and for tomato puree 19 samples were used with lycopene concentration ranging from 15.4 to 42.9 μg/g.

**Table 4.6: statistics of watermelon and tomato puree samples used for variable distance probe study**

| Sample set | No. of samples | Lycopene concentration of samples, μg/g | | |
|---|---|---|---|---|
| | | Mean | S.D. | Range |
| Watermelon puree | 21 | 33.0 | 11.3 | 11.2 - 57.7 |
| Tomato puree | 19 | 27.9 | 7.6 | 15.4 - 42.9 |

### *4.12.1 LS Regression for AI and NAI at various Distances between Fiber Optics*

The least squares regression for the absorbance index and normalized absorbance index of watermelon and tomato puree samples with lycopene concentration, at various distances between the emitter and detector fiber optics, were performed. The LS linear models for prediction of lycopene concentration from AI and NAI for various distances between fiber optics are presented in table 4.7. Slope of the linear models for AI decreased with an increase in the distance between the emitter and detector fibers for both watermelon and tomatoes. The NAI models for watermelon puree were almost parallel, whereas the slope of the tomato puree models increased with distance between fibers. This could be due to the higher light scattering by tomato puree than watermelon puree.

### *4.12.2 Multiple Regression for AI and NAI for watermelon and tomato puree*

Multiple regression models were developed for AI and NAI as a function of fiber optics separation distance, lycopene concentration, and their interaction, for watermelon

and tomato samples. The models obtained for watermelon and tomato puree samples are presented in table 4.8.

**Table 4.7: Linear regression model and $R^2$ values for least squares regression of absorbance index with lycopene concentration. Y =lycopene concentration in μg/g, X= absorbance index**

| Sample set | Distance between fibers (mm) | Absorbance Index (AI) Model | $R^2$ | Normalized Absorbance Index (NAI) Model | $R^2$ |
|---|---|---|---|---|---|
| Watermelon | 1.5 | Y = 78.750X - 2.237 | 0.94 | Y = 143.32X – 0.856 | 0.92 |
| | 2.5 | Y = 63.427X - 2.165 | 0.91 | Y = 143.59X – 1.551 | 0.90 |
| | 3.0 | Y = 59.899X - 3.887 | 0.92 | Y = 147.54X – 3.287 | 0.91 |
| | 3.5 | Y = 51.115X - 2.376 | 0.93 | Y = 147.73X – 3.994 | 0.92 |
| | 4.0 | Y = 48.951X - 3.873 | 0.94 | Y = 147.38X – 4.662 | 0.92 |
| | 4.5 | Y = 46.337X - 4.692 | 0.94 | Y = 149.02X – 5.793 | 0.91 |
| | 5.0 | Y = 41.772X - 3.408 | 0.94 | Y = 145.22X – 5.564 | 0.91 |
| | 5.5 | Y = 41.774X - 5.179 | 0.94 | Y = 149.66X – 7.018 | 0.94 |
| Tomato | 1.5 | Y = 69.716X + 5.019 | 0.80 | Y = 46.521X+ 10.149 | 0.72 |
| | 2.5 | Y = 53.955X + 4.258 | 0.72 | Y = 53.458X + 8.505 | 0.63 |
| | 3.0 | Y = 50.847X + 3.227 | 0.73 | Y = 58.780X + 7.639 | 0.59 |
| | 3.5 | Y = 46.729X +2.000 | 0.80 | Y = 69.736X +4.575 | 0.71 |
| | 4.0 | Y = 44.137X + 0.442 | 0.81 | Y = 76.281X + 2.484 | 0.74 |
| | 4.5 | Y = 39.729X + 1.089 | 0.76 | Y = 78.786X + 1.916 | 0.76 |
| | 5.0 | Y = 38.325X - 0.629 | 0.80 | Y = 85.819X - 0.921 | 0.80 |
| | 5.5 | Y = 33.410X + 1.551 | 0.76 | Y = 81.730X + 0.792 | 0.76 |

**Table 4.8: Multiple regression models for absorbance index of watermelon and tomato puree by 1mm fiber optics probe. AI = Absorbance Index; NAI = Normalized Absorbance Index; dist = center to center distance between fiber optics, mm; lyco = lycopene concentration, μg/g.**

| Samples | Prediction variable | Model | $R^2$ |
|---|---|---|---|
| Watermelon puree | AI | AI = -0.01404 + 0.00774*lyco + 0.03633*dist +0.00273*lyco*dist | 0.95 |
| | NAI | NAI = -0.01146 + 0.00699*lyco + 0.01592*dist -0.00021*lyco*dist | 0.91 |
| Tomato puree | AI | AI = -0.05018 + 0.00774*lyco + 0.03633*dist +0.00273*lyco*dist | 0.88 |
| | NAI | NAI = -0.01116 + 0.01448*lyco + 0.01592*dist -0.00103*lyco*dist | 0.70 |

The coefficients of the AI models for watermelon and tomato puree were significant (P=0.0002 for dist, and P<0.0001 for lyco, and lyco*dist). The AI prediction model surfaces have been plotted in figures 4.22 and 4.23. The AI models were parallel to each other at all the levels of lycopene concentration and distances, with significant difference between the predicted Absorbance Index (P<0.0001).

The NAI models for watermelon and tomato puree were parallel in distance but non parallel in lycopene concentration, as shown in table 4.8 and figures 4.24 and 4.25. The differences in predicted NAI values for watermelon and tomato puree were larger at higher levels of lycopene concentration. The interaction of lycopene and distance was not significant for watermelon NAI model (P=0.2667). The coefficient of distance on NAI models for both watermelon and tomato were not significant at 99% confidence level, but significant at 95% confidence level (P=0.0122). The coefficients of lycopene were significant (P<0.0001) but different for watermelon and tomato models, therefore the models were non parallel in lycopene concentration.

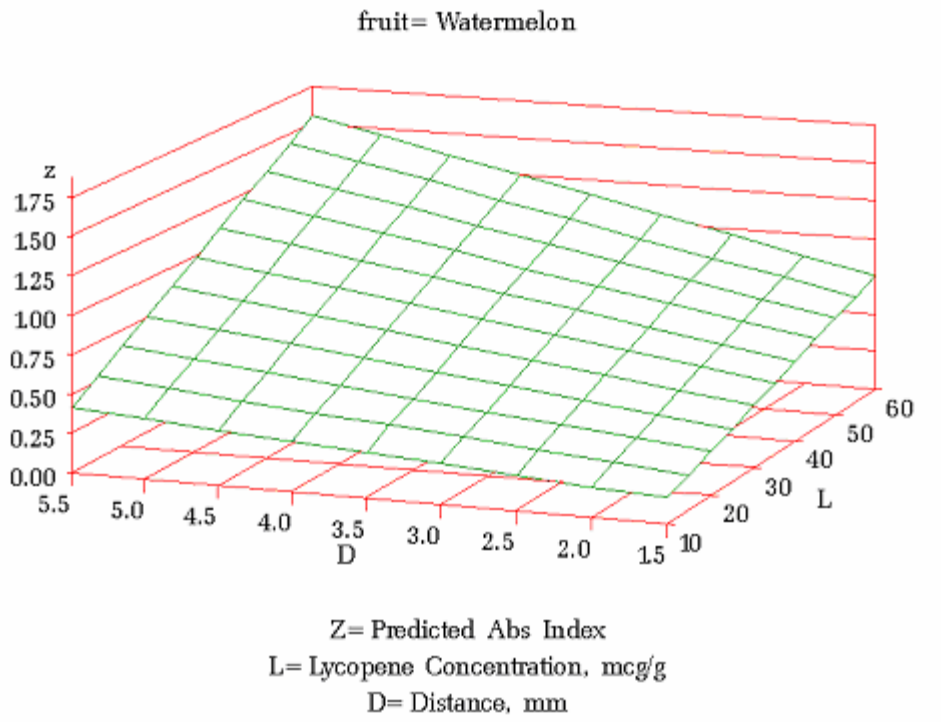


**Figure 4.22. Predicted AI response surface for watermelon puree samples**

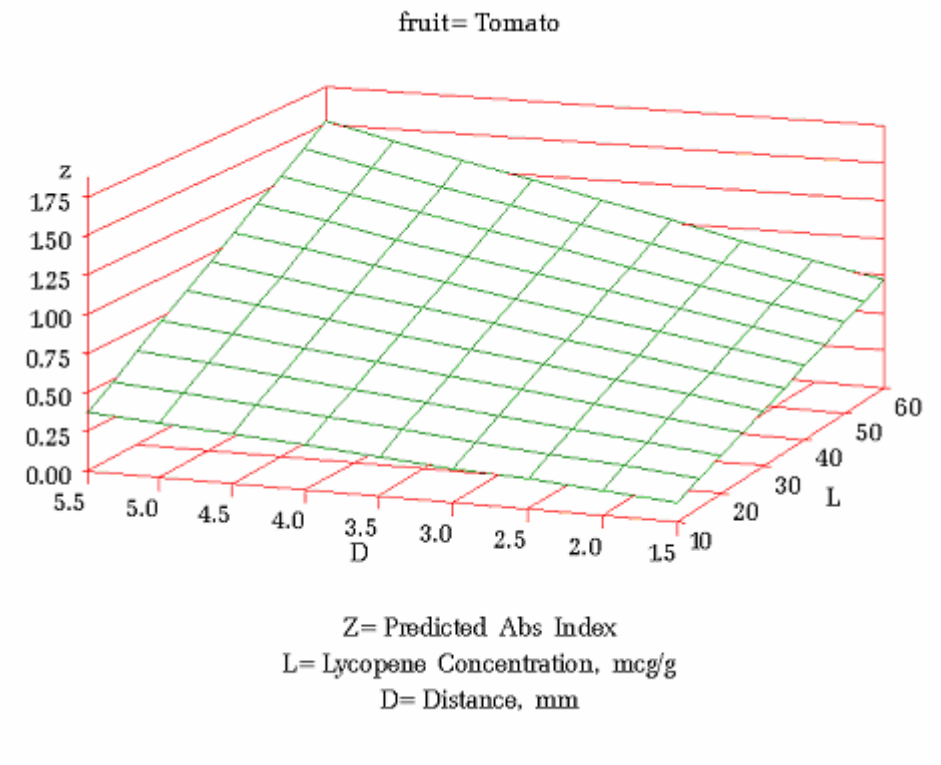


**Figure 4.23. Predicted AI response surface for tomato puree samples**

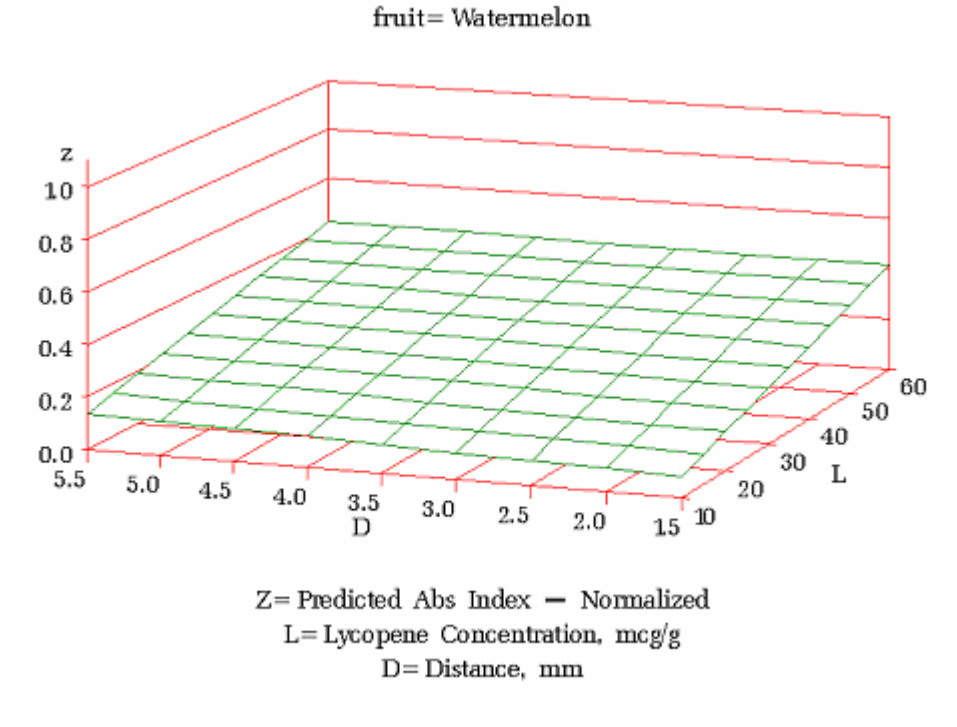


**Figure. 4.24. Predicted NAI response surface for watermelon puree samples**

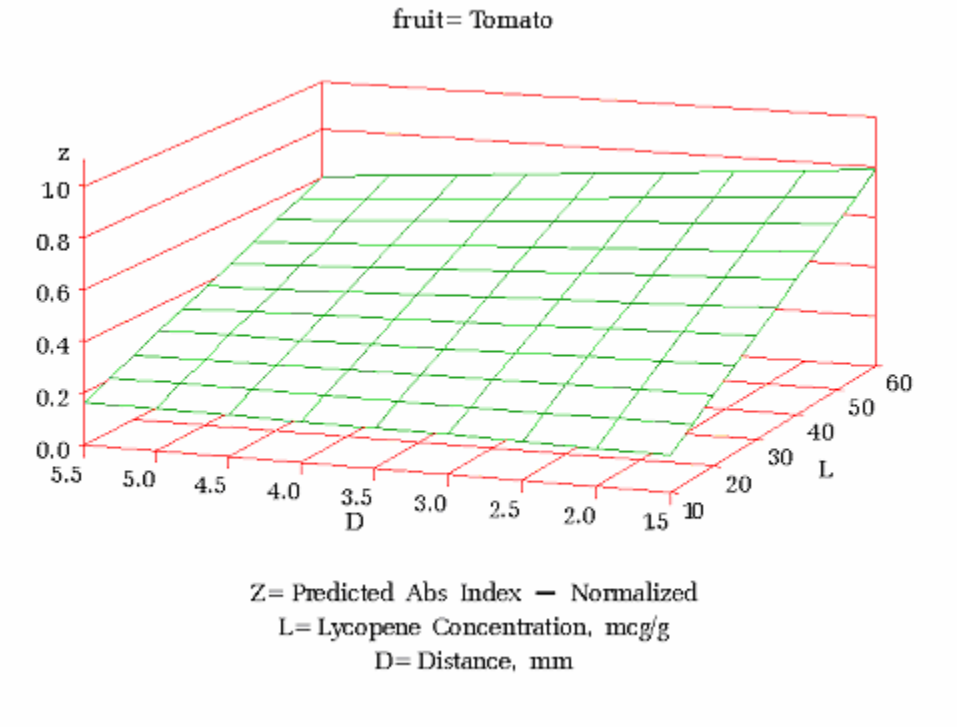


**Figure. 4.25. Predicted NAI response surface for tomato puree samples**

The models for AI and NAI for both fruits were significantly different than each other. Therefore the fiber optic probe must be calibrated for each fruit to estimate lycopene concentration.

A lower $R^2$ value was obtained for the tomato puree models. This may be attributed to the higher concentration of scattering particles such as seed and peel particles as compared to watermelon puree which was free from seed and peel. If the particulates of tomato samples were homogenized, the predictability of lycopene concentration in tomato puree samples may be enhanced.

### 4.13 CONCLUSIONS FROM VARIABLE DISTANCE PROBE STUDY

The multiple regression models for the Absorbance Index and Normalized Absorbance Index as a function of lycopene concentration (μg/g) and center-to-center distance (mm) between the light emitter and detector fiber optics, were significantly different between the type of fruits. There was a significant effect of distance between the fiber optics on the AI ($P<0.0001$) and slight effect on the NAI ($P=0.0122$). A fiber optic reflectance probe should be calibrated before used for a particular type of fruit.

# 5 CONCLUSIONS

## 5.1 SUMMARY

Watermelon and tomato are the major natural sources of lycopene, an important nutraceutical known for its effectiveness in preventing cancer and cardiovascular disease. The present methods of lycopene quantification in these fruits rely on a tedious process of lycopene extraction in hazardous organic solvents, followed by use of spectrophotometer or HPLC. A faster and safer method is needed to simplify the quantification of lycopene in these fruits and eliminate the use of hazardous solvents.

We have attempted to develop rapid sensing techniques by correlating visible spectra of fruit tissues and pureed samples with their lycopene concentration. Fiber optics probes were used with a miniature spectrometer to obtain visible spectra of samples. A tungsten halogen lamp was used as a light source and an Ocean Optics S2000 fiber optic spectrometer was used to acquire spectra of samples in the visible wavelength range of 500 to 750 nm.

The first objective was to develop a correlation between visible spectra of watermelon flesh samples and their lycopene concentration so that lycopene concentration could be estimated directly from intact tissue of watermelon. Both transmittance and reflectance mode of spectra acquisition were used and compared. For transmittance mode, thin slices (2 mm thick) of watermelon flesh were used as samples. An Absorbance Index (AI) and a Normalized Absorbance Index (NAI) were developed

by using the absorbance at 565 nm and 700 nm. Reflectance spectra of 2 cm watermelon flesh cubes were acquired using a bifurcated fiber optics reflectance probe and a multivariate PLS regression model was developed to predict lycopene concentration.

Due to the high error of lycopene concentration predicted in watermelon flesh, our next attempt was to puree watermelon and tomato, to increase sample homogeneity. The bifurcated fiber optic reflectance probe was used to acquire reflectance spectra of the pureed samples and develop LS and PLS models for lycopene estimation.

Since it was easier to acquire reflectance spectra by a fiber optic reflectance probe, further study was conducted to find the effect of the distance between light emitter and detector optical fibers and lycopene on absorbance index. A fiber optic probe system was assembled to position two fiber optics of 1mm diameter in various distances in parallel to each other for conveying and receiving light through samples. Least squares (LS) regression was used for correlation of AI and NAI with lycopene concentration at various distances between fiber optics. Multiple regression models for the AI and NAI as a function of lycopene concentration (μg/g) and center to center distance (mm) between light emitter and detector fiber optics were developed for watermelon and tomato puree samples.

The following conclusions were drawn from the results of the study:

1. The absorbance index (AI) and normalized absorbance index (NAI) obtained from transmittance data (by subtracting absorbance at 700nm from that at 565nm) had linear correlation with lycopene concentration of watermelon flesh ($R^2$ = 0.67 for AI and 0.66 for NAI). This information could be used for

design of an optical sensor for estimating lycopene concentration in watermelon flesh.

2. The PLS regression model from reflectance spectra of watermelon flesh had a coefficient of determination of $R^2 = 0.94$ with a standard error of prediction (SEP) of 5.22 microgram of lycopene per gram (µg/g). This model was not as precise as the reference method, but could be used for rapid classification of watermelon into categories of 'low', 'medium' or 'high' lycopene concentration.
3. Both AI and NAI from reflectance spectra of watermelon and tomato puree had linear correlation with lycopene concentration ($R^2 = 0.90$ for AI and NAI from watermelon, and $R^2 = 0.62$ for AI and 0.61 for NAI from tomato) with nearly same coefficients of determination.
4. The Least Squares (LS) linear regression model from reflectance spectra of watermelon puree predicted lycopene concentration with an $R^2$ of 0.93, and an SEP of 5.1µg/g. The LS linear regression model for reflectance spectra of tomato puree predicted lycopene concentration with an $R^2$ of 0.54 and a SEP of 5.2µg/g.
5. The PLS regression models developed for watermelon and tomato puree, using a wavelength range of 500-750 nm had an $R^2$ of 0.97 and 0.93 respectively.
6. The PLS model for reflectance spectra of watermelon puree predicted lycopene concentration with an $R^2$ of 0.97 and a SEP of 3.4µg/g. The PLS

model for tomato puree could predict lycopene concentration with an $R^2$ of 0.88 and a SEP of 2.5μg/g.

7. The PLS regression models for watermelon and tomato puree could be used for rapid estimation of lycopene in watermelon and tomato puree samples. This method has a high practical significance for on-site or online sensing of lycopene concentration in product lines requiring continuous monitoring of lycopene concentration.
8. Multiple regression models for the Absorbance Index (AI) as a function of lycopene concentration (μg/g) and center to center distance (mm) between light emitter and detector fiber optics had an $R^2$ value of 0.95 for watermelon puree samples and 0.88 for tomato puree samples.
9. Multiple regression models for the Normalized Absorbance Index (NAI) as a function of lycopene concentration (μg/g) and center to center distance (mm) between light emitter and detector fiber optics had an $R^2$ value of 0.91 for watermelon puree samples and 0.70 for tomato puree samples.
10. The multiple regression models for tomato and watermelon were significantly different than each other for AI and NAI models. The AI models for tomato and watermelon were parallel to each other whereas the NAI models were non parallel in lycopene and parallel in distance.

## 5.2 SUGGESTIONS FOR FUTURE RESEARCH

Some additional information is required to design an accurate fiber optic reflectance sensor for quantification of lycopene concentration in pureed samples of fruits, foods and nutraceutical materials. Simple linear regression models based on

Absorbance Index (AI) and Normalized Absorbance Index (NAI) would be easier to implement when developing a lycopene sensor. A better linear regression could be found between the absorbance index and lycopene concentration if variables affecting the absorbance index, other than lycopene, could be found. It was observed that the intensity of the light source affected the absorbance index. The following recommendations may be considered for design of a lycopene sensor:

1. The effect of the intensity of a light source and the diameter of an optical fiber on the AI and NAI should be evaluated to determine optimum light intensity and fiber diameter.
2. A dark sample chamber may be designed to avoid the effect of ambient light on visible spectra from samples.
3. Effect of particle size and concentration of fibers, and seed particles on absorbance index of puree samples may be evaluated to improve the precision of optical sensing of lycopene.
4. Hyperspectral images of cut watermelons and whole tomatoes may be used to estimate lycopene concentration by calibration of image features with lycopene concentration. This method should give better results compared to a correlation based on spectrum acquired from a small area by a fiber optic reflectance probe.
5. Pulsed laser light sources may be used to avoid fluctuation in ambient light conditions in the spectra of samples. Response from lasers at 565 nm and 700 nm may be evaluated by correlating the absorbance index with lycopene concentration.

# REFERENCES


Adsule, P.G., and A. Dan. 1979. Simplified extraction procedure in the rapid spectrophotometric method for lycopene estimation in tomato. *J. Food Sci. and Techno.l* 16:216-218.

Agarwal S. and A.V. Rao. 2000. Tomato lycopene and its role in human health and chronic disease. *CMAJ* 163(6):739-744.

Anon. 2004. Online course on "UV-Visible absorption spectroscopy, theoretical principles". Available at http://www.shu.ac.uk/schools/sci/chem/tutorials/molspec/uvvisab1.htm

Arias, R., T.C. Lee, L. Logendra and H. Janes. 2000. Correlation of lycopene measured by HPLC with the L*, a*, b* color readings of a hydroponic tomato and the relationship of maturity with color and lycopene content. *J. Agr. Food Chem.* 48:1697-1702.

Astorg, P. 1997. Food carotenoids and cancer prevention: An overview of current research. *Trends Food. Sci. Technol.* 8:406-413.

Beerh, O., and G. Sidappa. 1959. A rapid spectroscopic method for the detection and estimation of adulterants in tomato ketchup. *Food. Technol.*13: 414-418.

Boileau T.W., A.C. Boileau, and J.W. Jr. Erdman. 2002. Bioavailability of *all-trans* and *cis*-Isomers of Lycopene. *Exp Biol Med* 227:914-919.

Bolt, R.A., and J.J. Ten Bosch. 1993. Methods for measuring position-dependent volume reflection. *Appl. Optics*. 32 (24):4641-4645.

Britton, G. 1995a. Structure and properties of lycopene in relation to function. *FASEB J*. 9:1551-1558.

Britton, G. 1995b. UV/Visible spectroscopy. In Carotenoids:spectroscopy. Britton, G., S. Liaaen-Jensen, and H. Pfander, eds. Vol. 1B, 13-62. Birkhauser, Basel.

Buiteveld, H., J. M. H. Hakvoort, and M. Donze. 1994. The optical properties of pure water. In *SPIE Proceedings on Ocean Optics XII*. Edited by J. S. Jaffe. 2258: 174-183.

Cadoni, E., M. R. De Giorgi, E. Medda, and G. Poma. 2000. Supercritical $CO_2$ extraction of lycopene and β-carotene from ripe tomatoes. *Dyes and Pigments*. 44:27-32.

Chau, F., Y. Liang, J. Gao, X. Shao. 2004. Chemometrics- from basics to wavelet transform. John Wiley and Sons, Inc., Hoboken, NJ.

Choudhary R., T.J. Bowser, P. Weckler, N.O. Maness, W. McGlynn, and M.L. Stone. 2004a. Rapid sensing of lycopene in watermelon and tomato by visible reflectance spectroscopy. Proceedings of the Research Symposium, Food and Agricultural Products Research and Technology Center, Oklahoma State University, Stillwater, OK. April 21, 2004.

Choudhary R., T.J. Bowser, P. Weckler, N.O. Maness, W. McGlynn, and M.L. Stone. 2004b. Estimation of lycopene concentration in watermelon and tomato puree by visible reflectance spectroscopy. Presented at the Annual International Meeting of the ASAE, Ottawa, Canada, Aug 1-4, 2004.

Clinton, S.K. 1998. Lycopene: Chemistry, biology, and implications for human health and disease. *Nutr. Rev.* 56:35-51.

Collins, J.K. 2003. Bioavailability and antioxidant protection of lycopene from watermelon. Unpublished M.S. Thesis, Oklahoma State University, Stillwater, OK.

Craft N.E. 1992. Carotenoid reversed-phase high-performance liquid chromatography methods: reference compendium. *Meth. Enzymol.* 213: 185-205.

Crofcheck, C.L., F.A. Payne, C.L. Hicks, M.P. Menguc, S.E. Nokes. 2002. Fiber optic sensor response to high levels of fat in cream. *Transactions of the ASAE.* 45(1):171-176.

D'Souza, M., S. Singh, and M. Ingle. 1992. Lycopene concentration of tomato fruit can be estimated from chromaticity values. *Hort. Sci.* 27 (5)465-466.

Dahm, D.J., and K.D. Dahm. 2001. Chapter 1: The Physics of Near Infrared Scattering. In *Near Infrared Technology in the Agricultural and Food Industries*, 39-58. P. Williams and K. Norris., eds. St. Pal, MN.: American Association of Cereal Chemists, Inc.

Davies, B. H. 1976. Carotenoids. In *Chemistry and Biochemistry of Plant Pigments.* Vol. 2. Goodwin, T. W. Academic Press, London.

Davis, A.R., W.W. Fish, and P. Perkins-Veazie. 2003a. A rapid hexane-free method for analyzing lycopene content in watermelon. *J. Food Sci.*68 (1): 328-332.

Davis, A.R., W.W. Fish, and P. Perkins-Veazie. 2003b. A rapid spectrophotometric method for analyzing lycopene content in tomato and tomato products. *Postharvest Biology and Technology.*28: 425-430.

Di Mascio P., S.P. Kaiser, and H. Sies. 1989. Lycopene as the most efficient biological carotenoid singlet oxygen quencher. *Arch Biochem Biophys.* 274:532-538.

Fish W.W., P. Perkins-Veazie, J.K. Collins. 2002. A quantitative assay for lycopene that utilizes reduced volume of organic solvents. *J. Food Comp. Anal*. 15:309-317.

Frei, R.W., and J.D. MacNeil, 1973. Diffuse reflectance spectroscopy in environmental problem solving. CRC Press, Cleveland, OH.

Gerster, H. 1997. The potential role of lycopene for human health. *J. Am. Coll. Nutr*. 16:109-126.

Giovannucci, E. 1999. Tomatoes, tomato-based products, lycopene, and cancer: review of the epidemiologic literature. *J. Natl. Cancer Inst.* 91(4): 317-331.

Giovannucci, E., A. Ascherio, E.B. Rimm, M.J. Stampfer, G.S. Colditz, and W.C. Willet. 1995. Intake of carotenoids and retinol in relation to risk of prostate cancer. *J. Natl. Cancer Inst.* 87:1767-1776.

Goodwin, T.W. 1980. The biochemistry of the carotenoids. Vol. 1: Plants. Chapman and Hall, NY. 33-76

Hadley, C.W., E.C. Miller, S.J. Schwartz, and S.K. Clinton. 2002. Tomatoes, lycopene, and prostate cancer: progress and promise. *Exp. Biol. Med.* 227:869-880.

Harris DA (1996). Light spectroscopy. Bios Scientific Publishers Limited, Oxford, UK.

Hruschka, W.R. 2001. Chapter 3: Data Analysis: Wavelength Selection Methods. In: *Near Infrared Technology in the Agricultural and Food Industries*, 39-58. P. Williams and K. Norris., eds. St. Pal, MN.: American Association of Cereal Chemists, Inc.

Ishida B.K., J. Ma, and B. Chan. 2001. A simple, rapid method for HPLC analysis of Lycopene Isomers. *Phytochemical Analysis,* 12, 194-198.

Johnson, E.J. 2000. The role of lycopene in health and disease. *Nutrition in Clinical Care*. 3:35-43.

Kawamura, S., M. Nastuga, and K. Itoh. 1999. Determination of undried rough rice constituent content using near infrared transmission spectroscopy. *Trans. ASAE* 42(3): 813-818.

Kramer, R. 1998. Chemometric techniques for quantitative analysis. Marcel Dekker Inc. NY. 131-141.

Levy, J., E. Bosin, B. Feldman, Y. Giat, A. Munster, M. Danilenko, and Y. Sharoni. 1995. Lycopene is a more potent inhibitor of human cancer cell proliferation than either α or β-carotene. *Nutr. Cancer* 24:257-266.

Lu R., and D. Ariana. 2002. A near infrared sensing technique for measuring internal quality of apple fruit. *Trans. ASAE*. 18(5): 585-590.

Lu, R. 2001. Predicting firmness and sugar content of sweet cherries using near infrared diffuse reflectance spectroscopy. *Trans. ASAE*. 44(5): 1265-1271.

Lucier, G., and B.Lin. 2001. Factors affecting watermelon consumption in the United States. In *Vegetables and Specialties Situation and Outlook.* 287: 23-29. Economic Research Service, USDA.

Mangles, A.R., J.M. Holden, G.R. Beecher, M.R. Forman, and E. Lanza. 1993. Carotenoid content of fruits and vegetables: An evaluation of analytic data. *J. Amer. Diet. Assoc.* 93:284-296

Masaev, M., R. Riemersma, J.M. Martin-moreno, J.K. Hutten, and F.J. Kok. 1997. Lycopene and myocardial infarction risk in the EURAMIC study. *Am. J. Epidemiol.* 146: 618-626.

Meeten, G.H., and P. Wood. 1993. Optical fiber methods for measuring the diffuse reflectance of fluids. *Meas. Sci. Technol*. 4:643-648.

MetaCyc Database. 2002. Available at: http://biocyc.org/META/new-image?type=PATHWAY&object=CAROTENOID-PWY&detail.

Morningstar D, Perkins-Veazie, PA, Rice, SA. 2003. Lycopene extraction from freeze-dried tomatoes. Poster presentation. Botany, Mobile, Alabama. Botanical Society of America. July 29, 2003.

Mortan, R.A. 1975. Biochemical spectroscopy. John Wiley, NY.p:166.

Nolan, D.A., P.E. Blaszyk, and E. Udd. 1991. Optical fibers. In *fiber optic sensors*. E.Udd, ed. John Wiley and Sons, Inc. NY. Pp 9-15.

Olson, J.A., and N.I. Krinsky. 1995. The colorful, fascinating world of the carotenoids: important physiologic modulators. *FASEB J*. 9:1547-1550.

Perkins-Veazie, P., J.K. Collins, S.D. Pair, and W. Roberts. 2001. Lycopene content differs among red-fleshed watermelon cultivars. *J. Sci. Food and Agr.* 81:983-987.

Rao, A.V., and S. Agarwal. 1999. Role of lycopene as antioxidant carotenoid in the prevention of chronic disease: A review. *Nutr. Res*. 19(2):305-323.

Ray, K., and T.N. Misra. 1997. Photophysical properties of lycopene organized in langmuir-blodgett films: formation of aggregates. *Journal of Photochemistry and Photobiology A: Chemistry*. 107: 201-205.

Ribayo-Mercado, J.D., M. Garmyn, B.A. Gilchrest, and R.M. Russell. 1995. Skin lycopene is destroyed preferentially over β-carotene during ultra-violet irradiation in humans. *J. Nutr*. 125:1854-1859.

Rost, 1996. Tomato anatomy. Available at: http://www-plb.ucdavis.edu/labs/rost/Tomato /Reproductive/anat.html.

Sadler G, J. Davis D. Dezman. 1990. Rapid extraction of lycopene and β-carotene from reconstituted tomato paste and pink grapefruit homogenates. *J. Food Sci*. 55: 1460-1461.

Scott, K.J. and D.J. Hart. 1995. Development and evaluation of an HPLC method for the analysis of carotenoids in foods, and the measurement of the carotenoid content of vegetables and fruits commonly consumed in the UK. *Food Chem*. 54:101-111.

Sharma, S.K. and M. Le Maguer. 1996. Lycopene in tomato and tomato pulp fractions. *Ital. J. Food Sci*. 49:1214-1218.

Shi J. and M. Le Maguer. 2000. Lycopene in Tomatoes: Chemical and physical properties affected by food processing. *Crit. Rev. Biotechnol*. 20(4):293-334.

Shi, J., M. Le Maguer, M. Bryan, and Y. Kakuda. 2003. Kinetics of lycopene degradation in tomato puree by heat and light irradiation. *Journal of Food Process Engineering*. 25(6): 485-498.

Silberberg, M.S. 2000. Chemistry: The molecular nature of matter and change. 2nd ed. McGraw-Hill Companies Inc.NY.

Simmons, E.L. 1975. Diffuse reflectance spectroscopy: a comparison of the theories. *Applied Optics*. 14(6): 1380-1386.

Stahl W., A.R. Sundquist, M. Hanusch, W. Schwarz, H. Sies. 1993. Separation of beta-carotene and lycopene geometrical isomers in biological samples. *Clin. Chem.* 39:810-814.

Tinker, J.H., F. Bohm, W. Schalch, and T.G. Truscott. 1994. Dietary carotenoids protect human cells from damage. *J. Photochem. Photobiol*. B, 26:283-285.

Tomes, M.L., K.W. Johnson, and M. Hess. 1963. The carotene pigment content of certain red fleshed watermelons. *Pro. Am. Soc. Hort. Sci. 82*: 460-464.

USDA. 2004. National Nutrient Database for Standard Reference, Release 16-1. Available at: http://www.nal.usda.gov/fnic/foodcomp/cgi-bin/list_nut_edit.pl

USDA-NASS. 2004. Agricultural Statistics Database. Available at http://usda.mannlib.cornell.edu/reports/nassr/fruit/pvg-bb/2004/vege0404.pdf

USDA-NCC. 1998. USDA-NCC Carotenoid Database for U.S. Foods-1998. Available at: http://www.nal.usda.gov/fnic/foodcomp/Data/car98/car_tble.pdf.

Weisburger, J.H. 1998. Evaluation of the evidence on the role of tomato products in disease prevention. *Proc. Soc. Exp. Biol. Med.* 218(2):93-94

Wendlandt, W.W., and H.G. Hecht.1966. Reflectance spectroscopy. John Wiley and Sons, NY.

Williams P., and K. Norris. 2001. Near Infrared Technology in the Agricultural and Food Industries. American Association of Cereal Chemists, Inc. St. Pal, MN.

Wolfbeis, O.S. 1991. Fiber optic chemical sensors and biosensors. Volume I. CRC Press Inc. Boca Raton, FL.

Zang, L.Y., O. Sommerburg, and F.J.G.M.van Kuijk. 1997. Absorbance changes of carotenoids in different solvents. *Free Radical Biology and Medicine*. 23(7):1086-1089.

## Appendix A – Overall error calculation for lycopene analysis by hexane extraction method

The lycopene concentrations in watermelon and tomato samples were calculated using the following equation:

$L = 3.14\ A\ H / S$ (1)

Where,

L = Lycopene concentration, μg/g

A = Absorbance of hexane extract

H = Volume of hexane used, mL

S = sample weight, g

The absorbance value, A, varied from 0.100±0.008 to 0.500±0.008

The sample weight, S, varied from 0.500±0.001g to 2.000±0.001g.

Volume of hexane, H, was 50±1mL

The overall error in L is calculated from equation 2 as follows:

$$E_L = \left|\frac{\partial L}{\partial A}\Delta A\right| + \left|\frac{\partial L}{\partial H}\Delta H\right| + \left|\frac{\partial L}{\partial S}\Delta S\right| \quad (2)$$

$\left|\frac{\partial L}{\partial A}\right|$ = 3.14 H/S = 3.14x50/2.000 to 3.14x50/1 = 78.5 to 157

$\left|\frac{\partial L}{\partial H}\right|$ = 3.14 A/S = 3.14x0.100/2 to 3.14x0.500/1 = 0.157 to 1.57

$\left|\frac{\partial L}{\partial S}\right|$ = 3.14 A H/$S^2$ = 3.14x0.100x50/$(2.000)^2$ to 3.14x0.500x50/$(1.000)^2$ = 3.93 to 78.5

Hence,

Minimum $E_L = (78.5)(0.008) + (0.157)(1) + (3.93)(0.001) = 0.79 \approx 0.8 \mu g / g$

Maximum $E_L = (157)(0.008) + (1.57)(1) + (78.5)(0.001) = 2.90 \approx 3 \mu g / g$

Therefore, we may expect an overall error of ±3 μg/g.

## Appendix B – Drawing of Sample Holder for Transmittance Spectra of Watermelon slice

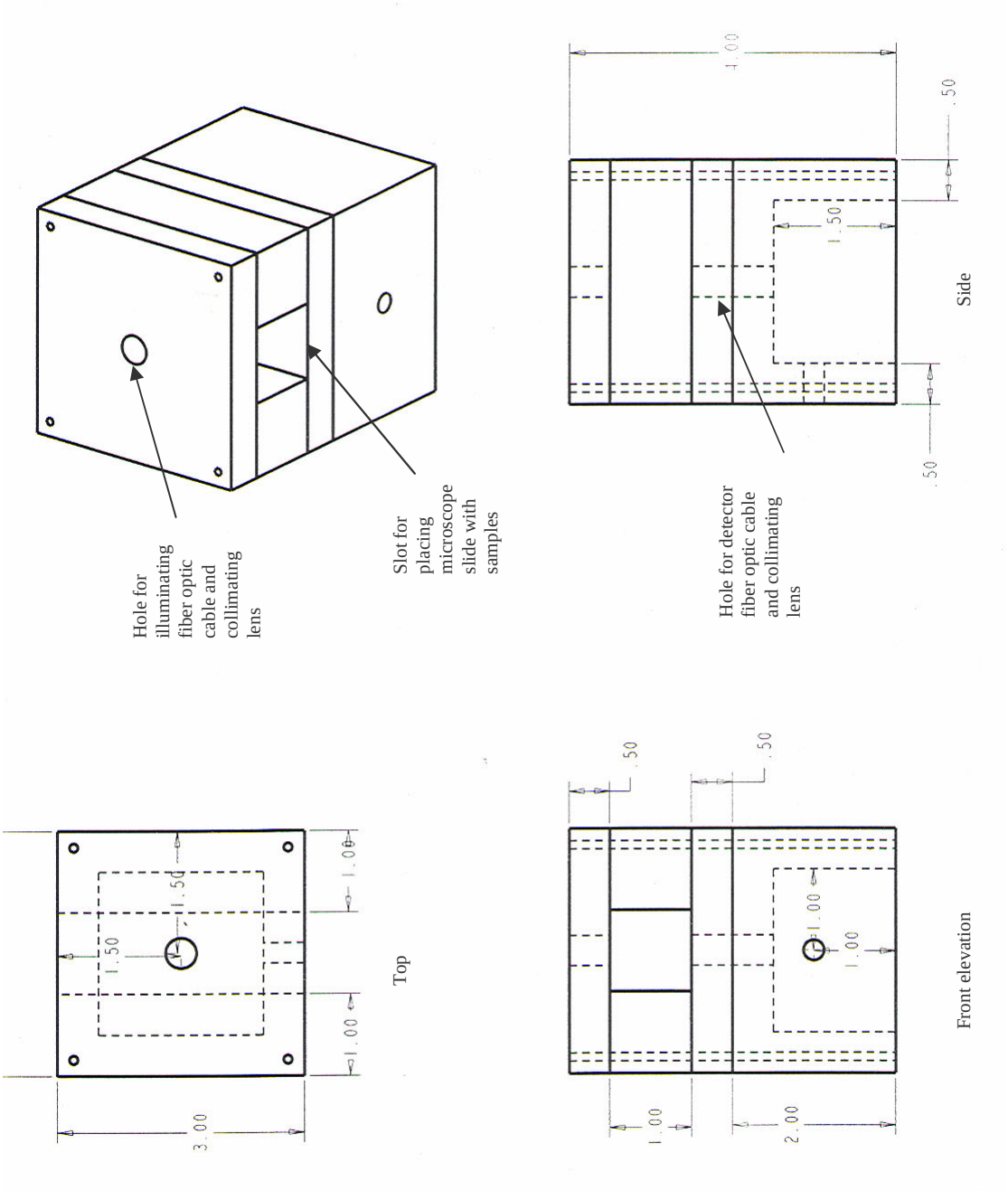

## Appendix C – Drawing of Variable Distance Fiber Optic Probe

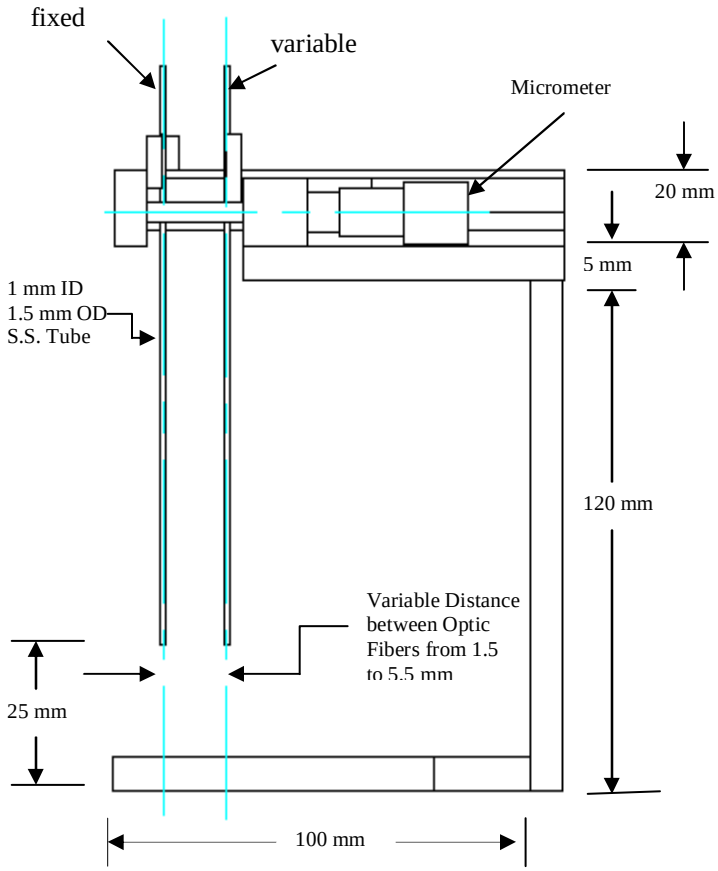


**Figure C1: Elevation of Variable Distance Fiber Optic Probe Assembly**

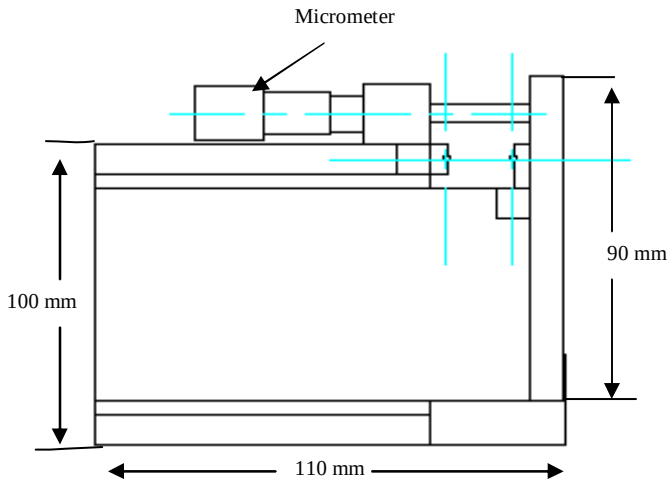


**Figure C2. Plan of Variable Distance Fiber Optic Probe Assembly**

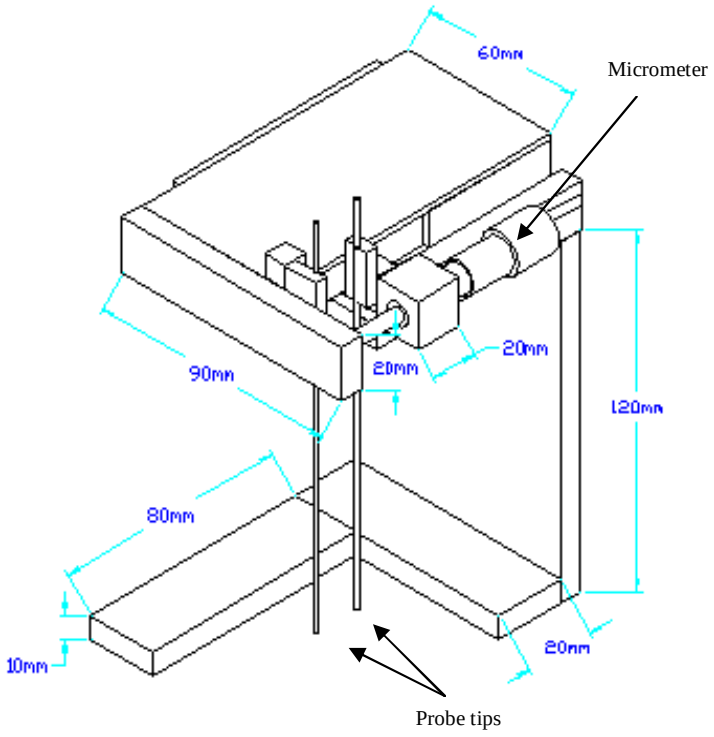


**Figure C3. Isometric View of Variable Distance Fiber Optic Probe Assembly**

# VITA

Ruplal Choudhary

Candidate for the Degree of

Doctor of Philosophy

Dissertation: RAPID ESTIMATION OF LYCOPENE CONCENTRATION IN WATERMELON AND TOMATO SAMPLES BY FIBER OPTIC VISIBLE SPECTROSCOPY

Major Field: Biosystems Engineering

Biographical:

Education: Higher secondary school certificate from Natwar High school, Raigarh, Chhattisgarh, India in June 1986; received Bachelor of Technology in Agricultural Engineering from Jawaharlal Nehru Agricultural University, Jabalpur, India in October 1991; received Master of Technology in Dairy and Food Engineering from Indian Institute of Technology, Kharagpur, India in January 1994; completed the requirements for the Doctor of Philosophy with a major in Biosystems Engineering at Oklahoma State University in December 2004.

Experience: Worked with Thapar Milk Products Limited, Alwar, India as Project Engineer, 1994; worked for Indian Institute of Technology, Kharagpur, as Research Scholar, 1994-1996; Employed by the Indian council of Agricultural Research as Scientist, and posted at Central Institute of Agricultural Engineering, Bhopal, 1996-1997; and at the National Dairy Research Institute, Karnal, India (1998-present on sabbatical). Worked as Graduate Research Associate at 'Biosystems and Agricultural Engineering Department', and 'Food and Agricultural Products Research and Technology Center', Oklahoma State University, Stillwater, OK, Aug 2001-Aug 2004.

Professional Affiliations: American Society of Agricultural Engineers, Association of Food Scientists and Technologists (India), Indian Society of Agricultural Engineers, Institute of Food Technologists, Sigma-Xi, the Scientific Honorary Society.